EASI SMR

D1.12 Pilot study with the LDR-50 district heating reactor

Rebekka Komu, Maria Oksa (VTT), Cristiano Ciurluini, Leonardo Bonaventura, Fabio Giannetti, Gianfranco Caruso (Sapienza University of Rome), Oleksandr Sevbo (Energorisk), Algirdas Kaliatka (LEI), Andrii Krushynskyi, Stanislav Sholomitsky (ARB)

1. Document information

Grant Agreement Number	n°101164810
Project Title	Ensuring Assessment of Safety Innovations for SMR
Project Acronym	EASI-SMR
Project Coordinator	Michael Montout, EDF
Project Duration	1 September 2024 – 31 August 2028 (48 months)
Related Work Package	WP1: Transverse topics for LW SMR acceptability and licensing
Lead Organisation	VTT
Contributing Partner(s)	Energorisk, LEI, Sapienza, ARB
Submission Date	15.6.2026
Dissemination Level	Public

2. History

Date	Submitted by	Reviewed by	Version (Notes)
15.6.2026	R. Komu	M. Oksa / M. Montout	V1 (initial)
29.06.2026	R. Komu	M. Montout	V2

Co-funded by the European Union

UK Research and Innovation

The Research Council of Norway

Project funded by

Table of Contents

List of Figures

List of Tables

3. Summary

This report presents a pilot study of the LDR lite district heating reactor within WP1 Task 1.5 of the EASI-SMR project, which addresses the safety and operational assessment of light-water SMRs in hybrid energy applications. The study provides a structured code-to-code benchmark of representative thermal-hydraulic analyses and demonstrates flexible operation of LDR lite, which is a public and simplified version of the LDR-50 reactor intended for research, education and benchmarking purposes. The benchmark covers hot full power steady state, station blackout (SBO), and small-break loss-of-coolant-accident (SBLOCA), and the load-follow operation is demonstrated with two representative 168-hour scenarios. System codes participating in the benchmark are Apros, RELAP5, ATHLET and COCOSYS, whereas the load-follow operation is demonstrated with coupled Apros-Ants.

The steady state results show generally good agreement in the main parameters, while larger differences are observed in quantities that are sensitive to nodalization and code-specific modelling approaches, such as heat losses. In the transient analyses, all the models predict that the reactor can be cooled passively during SBO, and that during the SBLOCA simulation the core remains covered without fuel or cladding heat-up. At the same time, notable differences can be seen in natural circulation flow rates, pressure evolution, break flow behaviour, and containment response highlighting areas where further model development and research is needed.

The load-follow analyses demonstrate stable reactor behaviour under varying district heating demand. The reactor tracks the power and supply temperature setpoints while the safety-relevant parameters remain below or at the initial levels. Overall, this study provides a useful basis for further model development, deeper investigation of the remaining discrepancies, and further safety assessment of LDR lite while supporting the feasibility of passive safety systems and flexible operation.

4. Keywords

LDR lite, LDR-50, SMR, district heating, benchmark, system code, SBO, SBLOCA, passive safety, load-follow

5. Abbreviations and acronyms

Acronym	Description
BOC	Beginning of cycle
CVCS	Chemical and volume control system
DHN	District heating network
HFP	Hot full power
LBLOCA	Large-break loss-of-coolant accident
LDR	Low temperature district heating reactor
PRZ	Pressurizer
SBO	Station blackout
SBLOCA	Small-break loss-of-coolant accident
SMR	Small Modular Reactor
TH	Thermal-hydraulic

Co-funded by the European Union
UK Research and Innovation
The Research Council of Norway
Project funded by

6. Introduction

This report presents a pilot study of the LDR lite district heating reactor carried out in the EASI-SMR project. The objective is to support the assessment of innovative light-water SMR concepts by providing a structured code-to-code comparison of representative thermal-hydraulic analyses. LDR lite is a public and simplified version of the LDR-50 reactor developed for research, education and benchmarking purposes.

The code-to-code benchmark evaluates how different system codes and modelling approaches reproduce the plant behaviour under common specifications. The benchmark covers hot full power steady state, station blackout (SBO) and small-break loss-of-coolant-accident (SBLOCA). In addition, flexible operation is demonstrated by modelling a representative load-follow scenario of 168 hours. Together these provide insight into the normal operation of the reactor as well as the passive safety response of the concept.

Co-funded by the European Union
UK Research and Innovation
The Research Council of Norway
Project funded by

7.LDR lite description

LDR lite (Komu, et al., 2025) is a small modular reactor (SMR) designed for low-temperature district heat production. The primary coolant flow is driven by natural convection in the integral design. Instead of conventional pressurizer, the reactor vessel is pre-pressurized with nitrogen, and the pressure follows the core outlet temperature. Heat is transferred to the district heating network (DHN) via secondary circuit, which is connected to the primary circuit via 16 shell-and-tube type heat exchangers.

The reactor vessel is enclosed inside the containment vessel, which is submerged in a pool. The containment vessel is partly filled with water, which opens up a heat transfer path from the primary circuit to the pool, which serves as the final heat sink. During normal operation the heat losses to the pool remain small, but as the primary temperature increases, the heat transfer is enhanced.

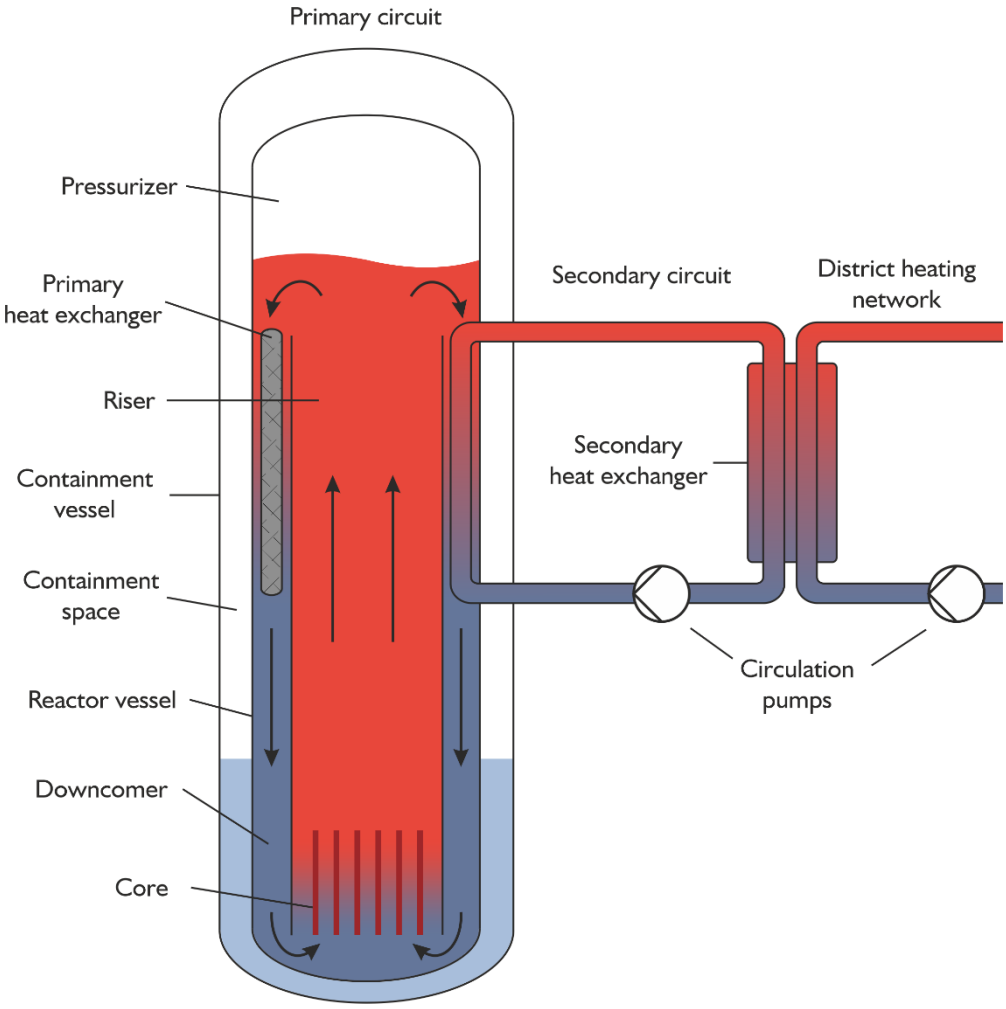

Figure 1. A schematic figure of the LDR lite module (Komu, et al., 2025).

8.Transient description

8.1. Steady state

Hot full power (HFP) steady state serves as the initial state for all transients. HFP state is reached by starting the calculation from cold state, defined in Table 1. The power is slowly increased to 100 % (for example in 3 hours) with the boundary conditions specified in Table 2. Steady state has been reached when the system has been stabilized.

Table 1. Cold state parameters (Komu, et al., 2025).

Parameter	Value	Unit	Note
Reactor power	0	MW	
PRZ pressure	0.1	MPa	pre-pressurized with nitrogen
Containment pressure	0.1	MPa	pre-pressurized with nitrogen
Primary circuit temperature	20	°C	
Containment water temperature	20	°C	
Pool temperature	20	°C	
Containment water level (elevation)	1.3447	m	
PRZ water level (elevation)	7.05	m	
Pool water level (elevation)	14.04	m	
Primary liquid mass	33748	kg	
Pressurizer nitrogen mass	8.2	kg	
Containment liquid mass	7411	kg	
Containment nitrogen mass	25.8	kg	

Table 2. Boundary conditions for HFP steady state (Komu, et al., 2025).

Parameter	Value	Unit	Note
Reactor power	50	MW	
Secondary circuit inlet	77	°C	
Secondary circuit outlet	125	°C	
Secondary circuit mass flow	245	kg/s	controlled to get outlet temperature
Secondary circuit pressure	1.5	MPa	
Pool temperature	30	°C	

8.2. SBO

During station blackout (SBO) transient, it is assumed that all power is lost and the reactor moves into passive decay heat removal mode. The transient begins after 100 seconds of steady state. The assumptions for the transient are as follows:

- The secondary circuit is lost: the pump stops and isolation valve in the cold leg closes
- Pool cooling stops allowing the pool to heat up
- All control rods drop into the core instantly as external power is lost, i.e. the reactor shifts to decay heat. The ANS-79 decay heat standard or the decay heat curve provided in the specifications can be used
- Simulation time is seven days (604 800 s)

The requested output is the time evolution of:

- Total reactor power (MW)
- Pressurizer pressure (MPa)
- Core inlet temperature (°C)
- Core outlet temperature after bypass (°C)
- Maximum fuel temperature (°C)
- Maximum cladding temperature (°C)
- Total primary mass flow rate (kg/s)
- Core mass flow rate (kg/s)
- Core bypass flow (kg/s)
- Containment pressure (MPa)
- Containment liquid temperature (°C)
- Heat losses to pool (kW)
- Pool temperature (°C)

8.3. SBLOCA

Due to the integral design, a large break loss of coolant accident (LBLOCA) is not possible in the LDR lite design. However, a small break loss of coolant accident (SBLOCA) is possible through the pipelines that penetrate the reactor vessel. One such line is the

chemical and volume control system (CVCS), which connects to the top of the heat exchangers.

The SBLOCA is modelled with the following assumptions:

- The CVCS line breaks at the reactor vessel connection point (see Figure 2)
- It is assumed that the CVCS line is isolated immediately, i.e. the CVCS system is not modelled, only direct leak from reactor vessel to the containment
- Reactor trip and secondary circuit isolation is activated by High containment pressure signal (> 2 bar)
- No pool cooling
- Simulation time is two hours (7200 s)
- No emergency coolant injections or other safety systems are activated

The requested output is the time evolution of:

- Total reactor power (MW)
- Pressurizer pressure (MPa)
- Core inlet temperature (°C)
- Core outlet temperature after bypass (°C)
- Core outlet boiling margin (°C)
- Maximum fuel temperature (°C)
- Maximum cladding temperature (°C)
- Total primary mass flow rate (kg/s)
- Core mass flow rate (kg/s)
- Core bypass flow (kg/s)
- Containment pressure (MPa)
- Containment liquid temperature (°C)
- Heat losses from reactor vessel to containment (kW)
- Heat losses from containment to pool (kW)
- Pool temperature (°C)
- Break liquid mass flow rate (kg/s)
- Break gas mass flow rate (kg/s)
- Integrated break mass flow (kg)
- Reactor vessel coolant mass, liquid+steam (kg)
- Reactor vessel nitrogen mass (kg)
- Reactor vessel collapsed liquid level elevation (m)
- Containment vessel coolant mass, liquid+steam (kg)
- Containment vessel nitrogen mass (kg)
- Containment vessel liquid level elevation (m)

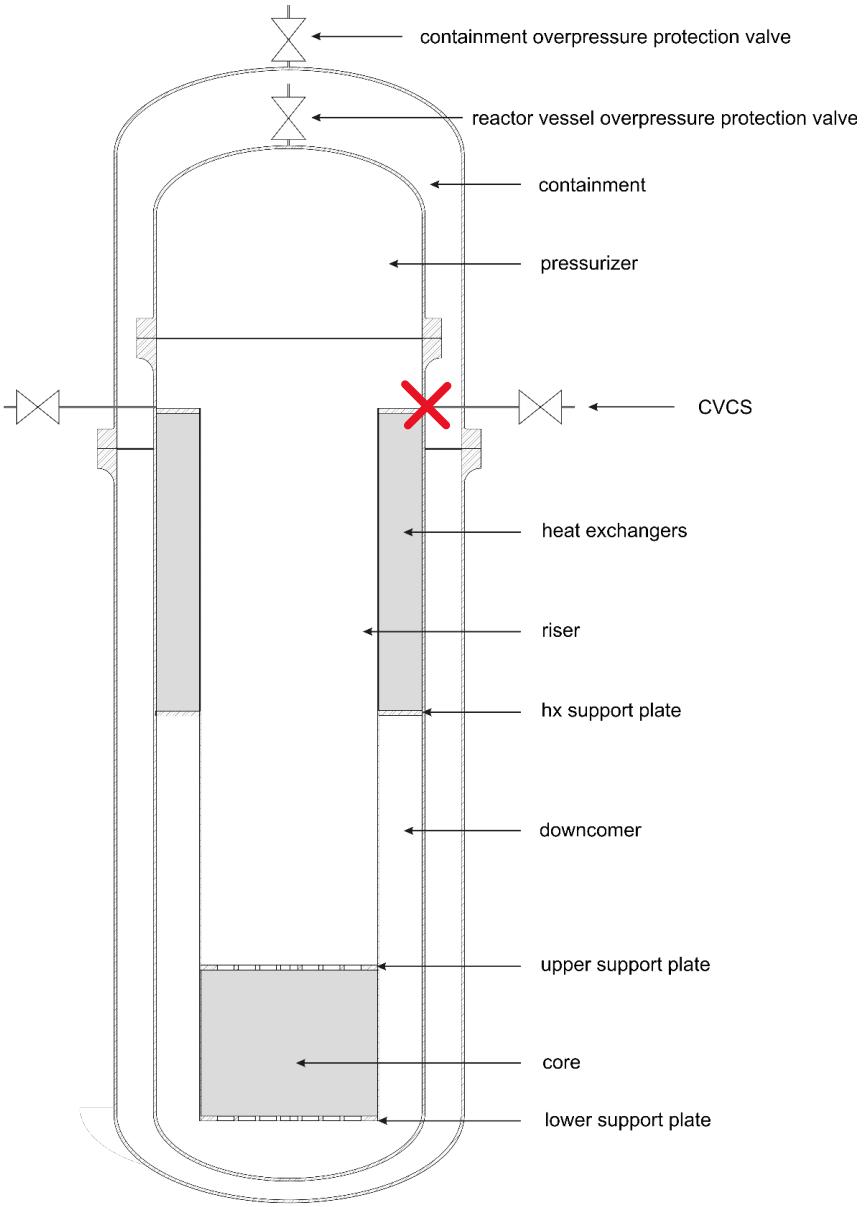

Figure 2. LDR lite module with the break location marked with red cross.

8.4. Load-follow

The load-following capability is demonstrated with two realistic 168-hour scenarios. The first scenario represents regular daily variation between 50 % and 100 % power (Scenario 1). The second scenario is based on historical weather and district heat demand data from Helsinki (Scenario 2). The district heating network sets boundary conditions for reactor power as well as supply temperature to the network and the returning coolant temperature. The boundary conditions for the two selected scenarios are presented in Figure 3.

Co-funded by the European Union
UK Research and Innovation
The Research Council of Norway
Project funded by

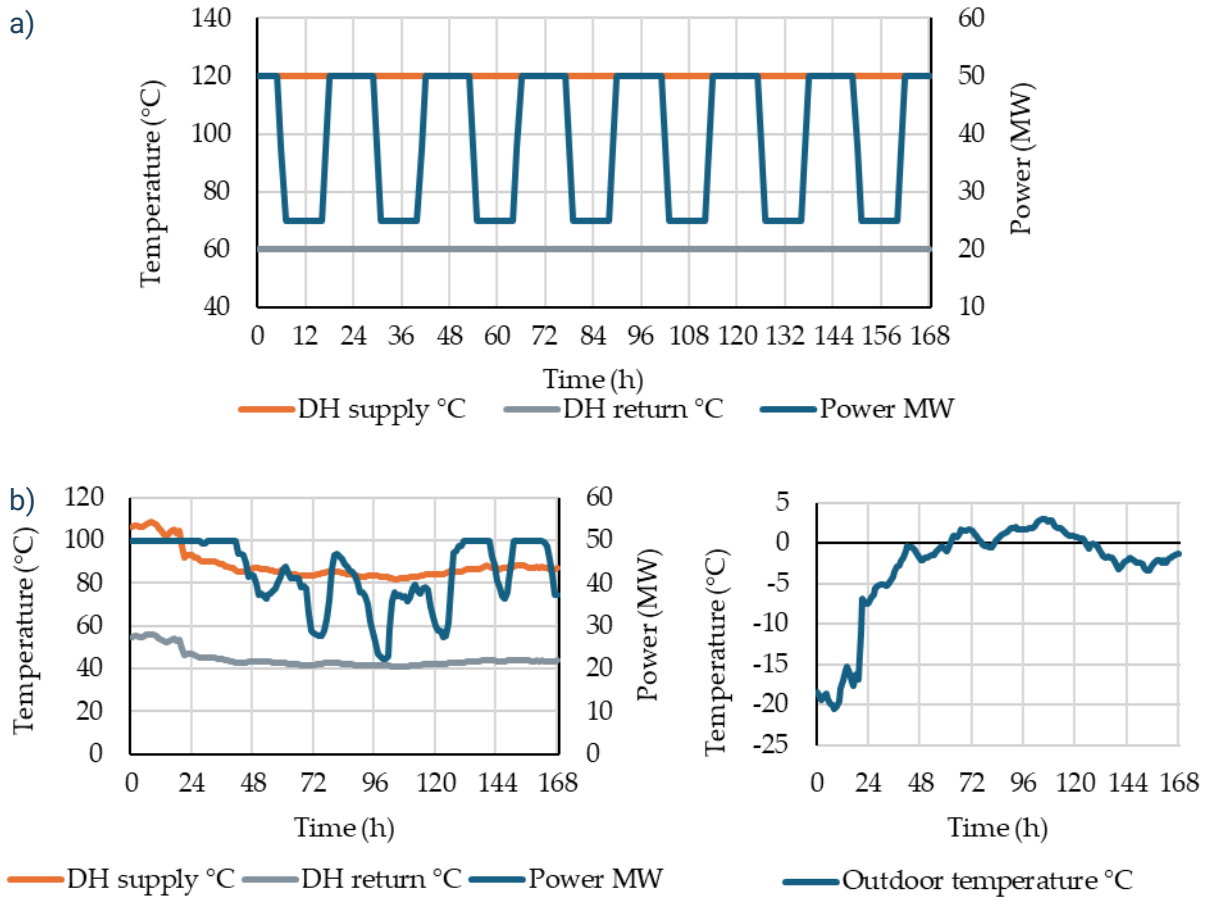

Figure 3. Boundary conditions for the load-follow demonstration cases: a) Scenario 1: regular daily variation between 50 % and 100 % power and b) Scenario 2: realistic scenario based on historical weather and district heat demand data in Helsinki (Komu, 2026).

In the control scheme, the reactor power is adjusted with control rods, while the secondary circuit temperatures remain constant. The hot leg temperature is controlled with the circulation pump speed, and the cold leg temperature is adjusted with the valve bypassing the district heating network heat exchanger. This way the temperature changes in the district heating network are not reflected in the primary circuit, creating stable boundary conditions for the core.

Co-funded by the European Union
UK Research and Innovation
The Research Council of Norway
Project funded by

9.Methods

In the code-to-code benchmark, the transient response of LDR lite was evaluated with respect to SBO and SBLOCA using thermal-hydraulic system codes. Five organizations participated in the benchmark. The organizations and the codes they used are presented in Table 3. The full descriptions of the codes and models can be found in Annex I.

Table 3. Organizations participating in the benchmark and their codes.

Organisation	Code	Note
VTT	Apros	
Sapienza	RELAP5	
LEI	RELAP5	
Energorisk	ATHLET	
ARB	COCOSYS	only containment

The load-follow scenarios were analyzed using only the Apros code coupled with nodal neutronics solver Ants (Rintala and Lauranto, 2023). The reactor core specifications for the beginning of cycle (BOC) were used. The Apros model is the same as described in Annex I with the exception of the core. The full model description can be found from (Komu, 2026).

10. Analysis of results

10.1. Steady state

The HFP steady state results are presented in Table 4. Standard deviation (SD) and coefficient of variation (CV) have been calculated for the results for comparison and to highlight the significant differences.

The primary circuit state is defined by how each code models the natural circulation with the given boundary conditions and loss coefficients. All models show similar mass flow rates with the LEI model predicting slightly higher temperatures. The primary pressure is set by the core outlet temperature and the nitrogen in the pressurizer showing good agreement. In the Sapienza model the temperature is slightly lower resulting in lower pressure. However, the biggest differences can be seen in steam and nitrogen masses. This might be due to differences in initialization of the model, how the codes model the gas space, or how users interpret the output.

The heat losses to containment are similar in VTT, Sapienza and LEI models, and Energorisk and ARB models. The ARB model gets boundary conditions from the Energorisk model, which explains the similar result. The differences between the results can be caused by different nodalization approaches or differences between the codes. Compared to the reactor power, the heat loss is around 0.5 %, which makes the differences minor at the whole system level.

Table 4. HFP steady state results.

Parameter	VTT (Apros)	Sapienza (RELAP5)	LEI (RELAP5)	Energorisk (ATHLET)	ARB (COCOSYS)	SD / CV (%)
Reactor power (MW)	50.0	50.0	50	50	_	0.00 / 0.00
Total HX power (MW)	49.779	49.83	49.81	49.02	_	0.34 / 0.69
Pressurizer pressure (MPa)	0.689	0.663	0.691	0.6898	_	0.01 / 1.71
Containment pressure (MPa)	0.107	0.115	0.1400	0.102	0.111	0.01 / 11.50
Core inlet temperature (°C)	103.46	101.2	109	103.98	_	2.85 / 2.73
Core outlet temperature (after bypass) (°C)	151.44	149.2	157	151.79	_	2.86 / 1.88
Total primary mass flow (kg/s)	244.46	244.55	243.55	243.1	_	0.61 / 0.25

Core bypass flow (kg/s)	12.72	12.86	8.87	1.17	_	4.74 / 53.28
Heat loss from primary to containment (kW)	231.79	240.6	244.6	187.6	187.237	25.61 / 11.73
Heat loss from containment to pool (kW)	230.60	240.6	243.3	187.5	189.3	24.75 / 11.34
Secondary circuit mass flow rate (kg/s)	245.39	245.0	245	245.48	_	0.22 / 0.09
Cold leg temperature (°C)	76.9	77.0	76.9	77.0	_	0.05 / 0.06
Hot leg temperature (°C)	125.0	125.2	125.1	125.02	_	0.08 / 0.06
Pool temperature (°C)	29.69	30.0	26.1	30.0	30.0	1.53 / 5.26
Pressure loss over core incl. upper and lower support plate (Pa)*	963.91	995.2	1010.0	1185.8	_	86.53 / 8.33
Pressure loss over primary heat exchanger (Pa)*	809.76		1900	1077.4	_	463.91 / 36.75
Primary collapsed water level (m)**	7.530	7.45	7.55	7.55	_	0.04 / 0.55
Containment collapsed water level (m)**	1.389	1.834	1.495	1.345	1.345	0.18 / 12.45
Pool collapsed water level (m)**	10.878	12.89	14.07	14.04	14.04	1.42 / 10.59
Primary liquid mass (kg)	33737	33743	33615	34270	_	252.75 / 0.75

Co-funded by the European Union
UK Research and Innovation
The Research Council of Norway
Project funded by

Primary steam mass (kg)***	12.663	0.333	7.93	6.82	_	5.22 / 105.28
Primary gaseous nitrogen mass (kg)	7.865	29.54	12.07	24.41	_	8.01 / 39.18
Primary dissolved nitrogen mass (kg)	-	This feature cannot be modelled in RELAP5	This feature cannot be modelled in RELAP5	n/a	_	
Containment liquid mass (kg)	7413	7380.4	6983.4	6468	7105	342.09 / 4.84
Containment steam mass (kg)***	0.168	0.013	-	0.565	0.193	0.20 / 86.37
Containment nitrogen mass (kg)	25.490	24.93	25.64	19.715	21.33	2.43 / 10.39
Pool liquid mass (kg)	998073	995772	998491	907386	906864	44258 / 4.60
*losses caused by loss coefficient and friction, excluding hydrostatic pressure						
**in elevation, not from structure bottom						
***water vapor, excluding non-condensable gases						

10.2. SBO

The results from the code-to-code comparison of the station blackout transient are presented in this section. The transient begins with the isolation of the secondary circuit and reactor trip, after which only decay heat remains (Figure 4). Following scram, the core inlet and outlet temperatures (Figure 5 and Figure 6) stabilize close to each other and the core mass flow rate (Figure 7) decreases.

Apros (VTT) and RELAP5 (LEI) predict similar mass flow rates whereas ATHLET (Energorisk) predicts slightly higher mass flow rate. The other RELAP5 model (Sapienza) shows a significantly lower primary mass flow rate. This aspect has been further investigated by comparing the nominal pressure drops profile along the primary circuit (see Table 4) and the axial heat flow profile along the RPV walls (RPV to containment heat losses). These two aspects seem aligned in VTT and Sapienza simulations. This means that the height difference between heat source and heat sink (i.e., natural circulation driving force) should be comparable. The same is valid for hydraulic resistance (i.e., pressure drops in Table 4). Since the natural circulation mass flow results from the balance of these two aspects, it should be comparable. To better understand this deviation, deeper investigations are needed.

Most of the models predict a slight increase in the primary temperature at the beginning of the transient, which is reflected on the primary pressure (Figure 8). As the transient progresses, the differences in the primary temperatures can be as high as ten degrees. VTT and LEI models have good agreement in the core outlet temperature, whereas the Sapienza and Energorisk models predict higher temperatures. In the VTT model, the primary pressure follows the core outlet temperature and drops close to 3 bars in a couple of days, but in other models the pressure decreases more slowly or remains high. This suggests that the other models, especially Sapienza and Energorisk, predict more coolant stratification in the pressurizer and less cooling. On the other hand, the models also show more nitrogen in the pressurizer in steady state, which might explain the differences. In these two models the pressure remains close to 6 bars.

The heat transfer through the containment to the pool (Figure 9) increases during the first couple of days due to the increased downcomer temperature and stabilizes to the same level as the reactor power. From the results it can be seen that the passive decay heat removal is enough to cool down the reactor during SBO without any fuel or cladding heat-up (Figure 10 and Figure 11). During the first week, the containment liquid temperature remains below boiling point and the pool temperature increases around 30 degrees (Figure 12).

LEI performed the investigation of containment nodalization influence on calculation results: the containment was modeled as a single element and as two paths, where two parallel pipe elements with crossflow were used. In the first case the heat from the reactor into water pool through the gap between reactor vessel and containment vessel is transferred only by conduction. In second case, because the nodalization allows the coolant mixing in containment, the heat is transferred not only by conduction, but also by coolant convection. This slightly increases the heat transfer through the gap between reactor and containment vessels. This change is reflected in the heat transfer from the containment to the water pool (as it is shown in Figure 13). However, this very insignificant change in heat losses into water pool has significant influence in pressurizer pressure (see Figure 14). There might be also other mechanisms affecting the pressure behavior in addition to the heat loss.

Co-funded by the European Union
UK Research and Innovation
The Research Council of Norway
Project funded by

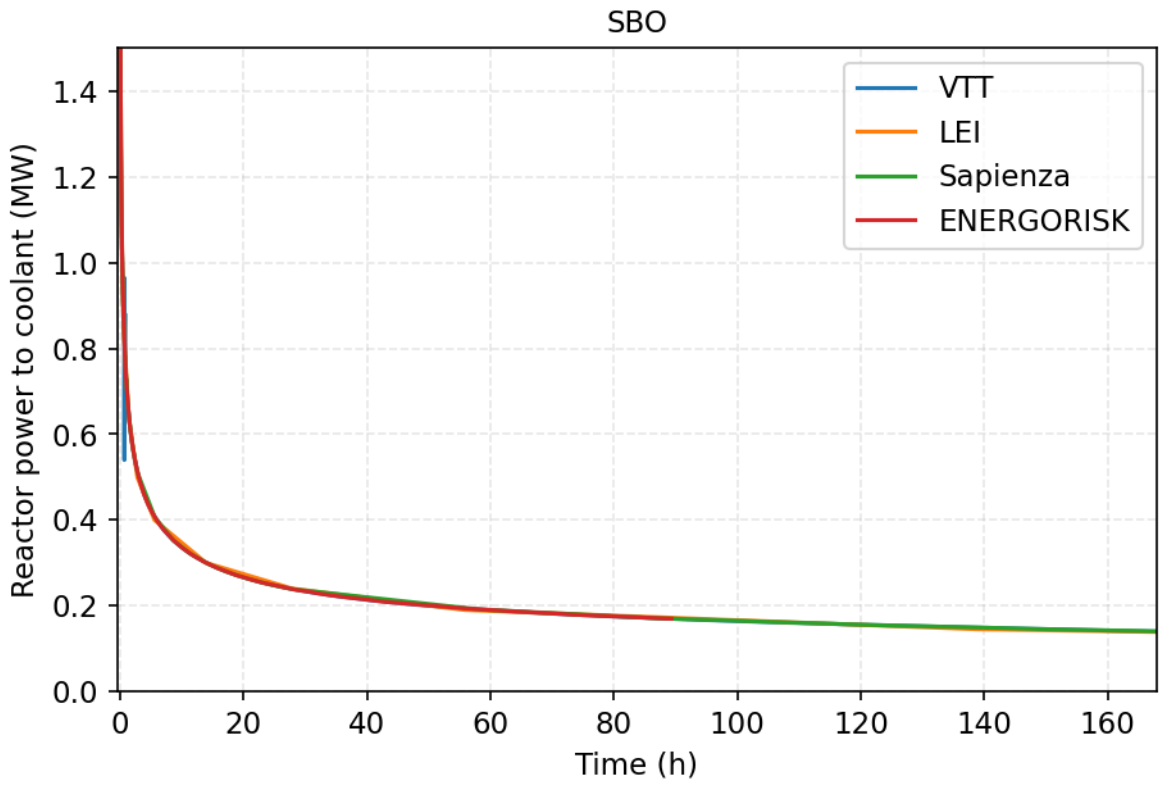

Figure 4. Reactor power during SBO transient (y-axis cropped for clarity).

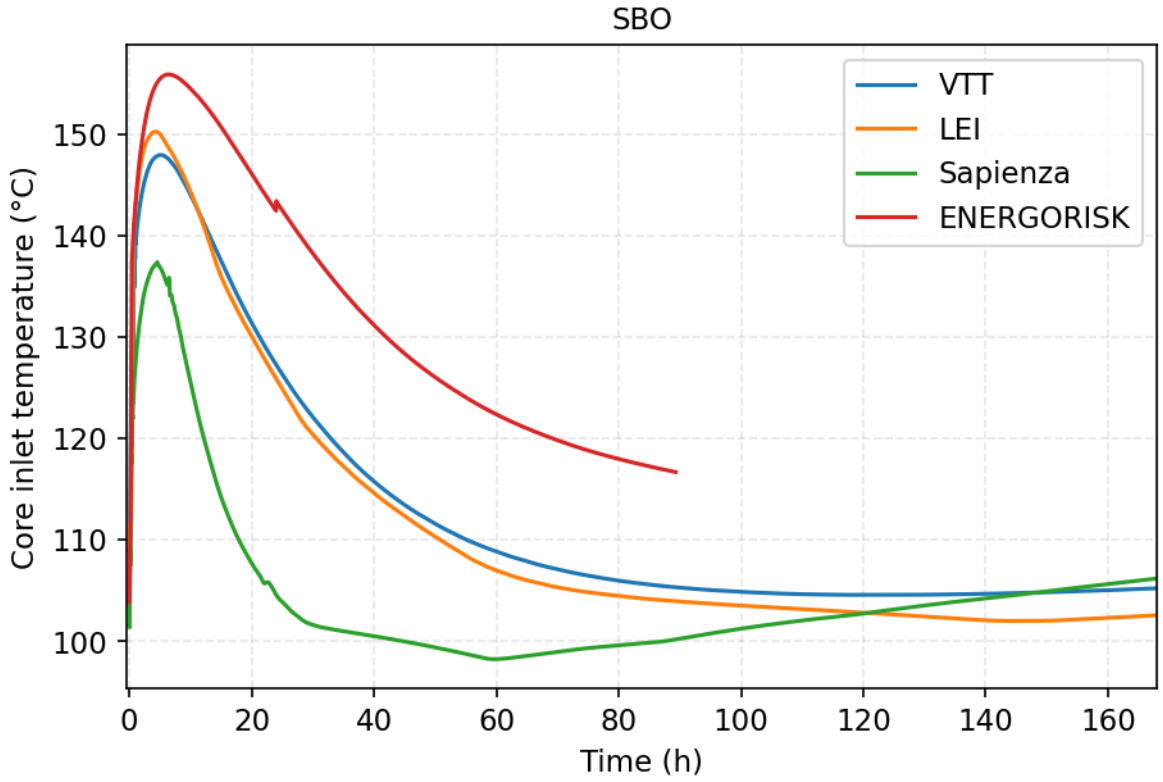

Figure 5. Core inlet temperature during SBO transient.

Co-funded by the European Union
UK Research and Innovation
The Research Council of Norway
Project funded by

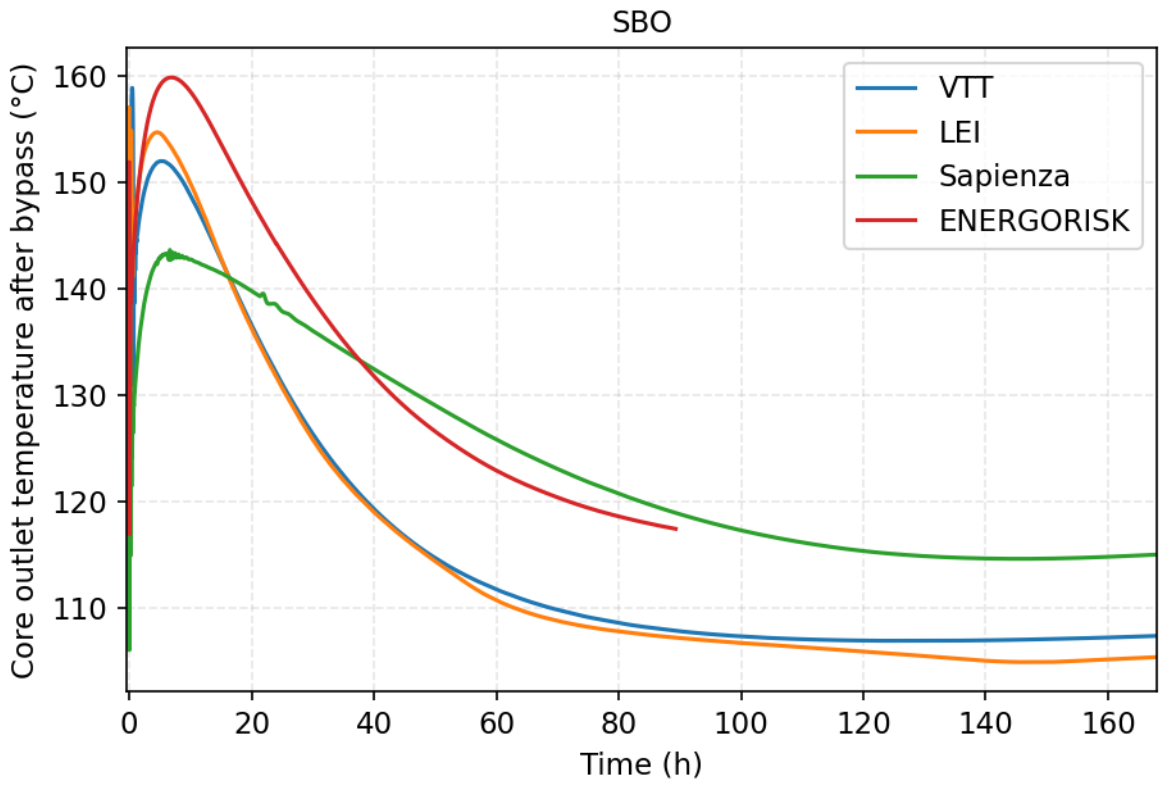

Figure 6. Core outlet temperature during SBO transient.

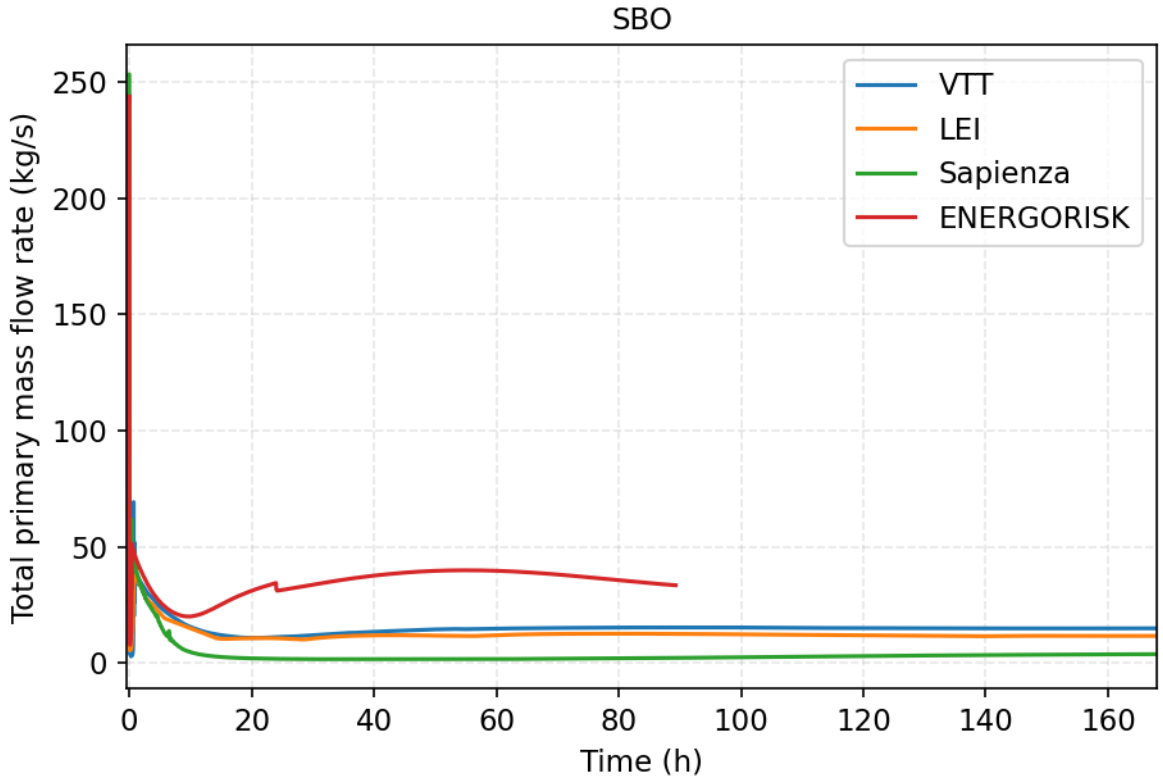

Figure 7. Total primary mass flow rate during SBO transient.

Co-funded by the European Union
UK Research and Innovation
The Research Council of Norway
Project funded by

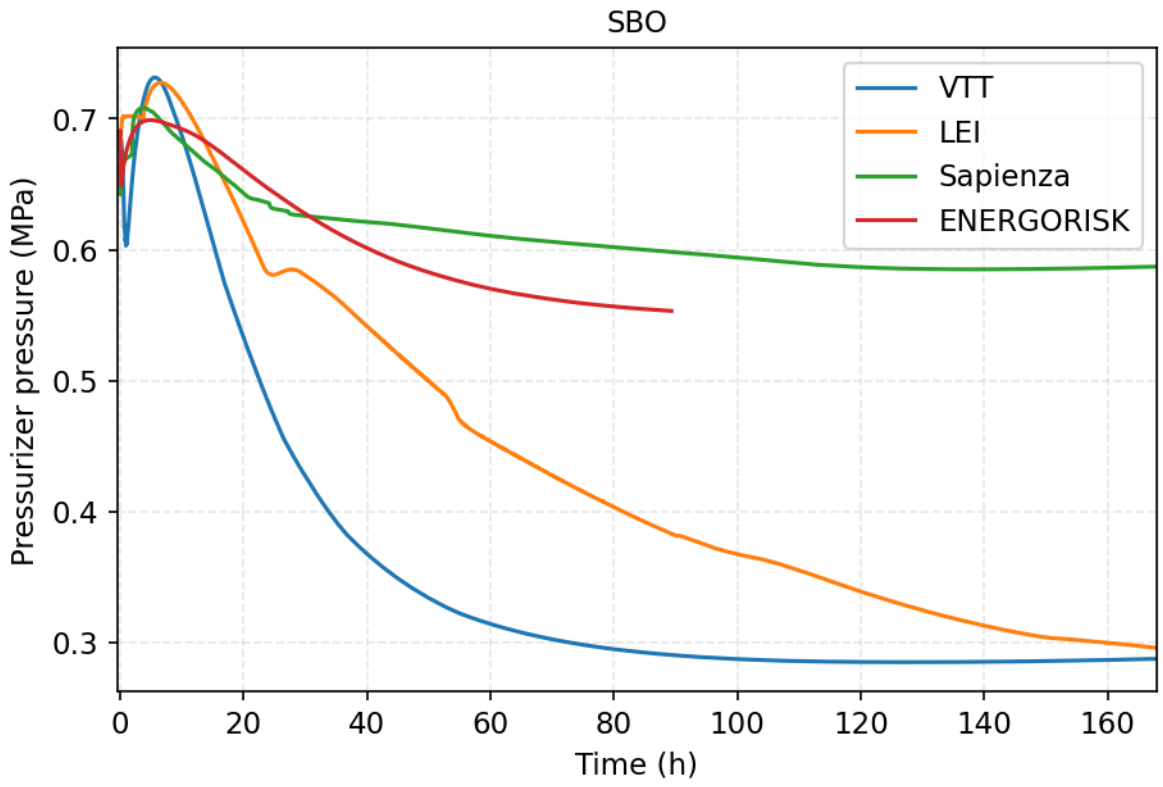

Figure 8. Pressurizer pressure during SBO transient.

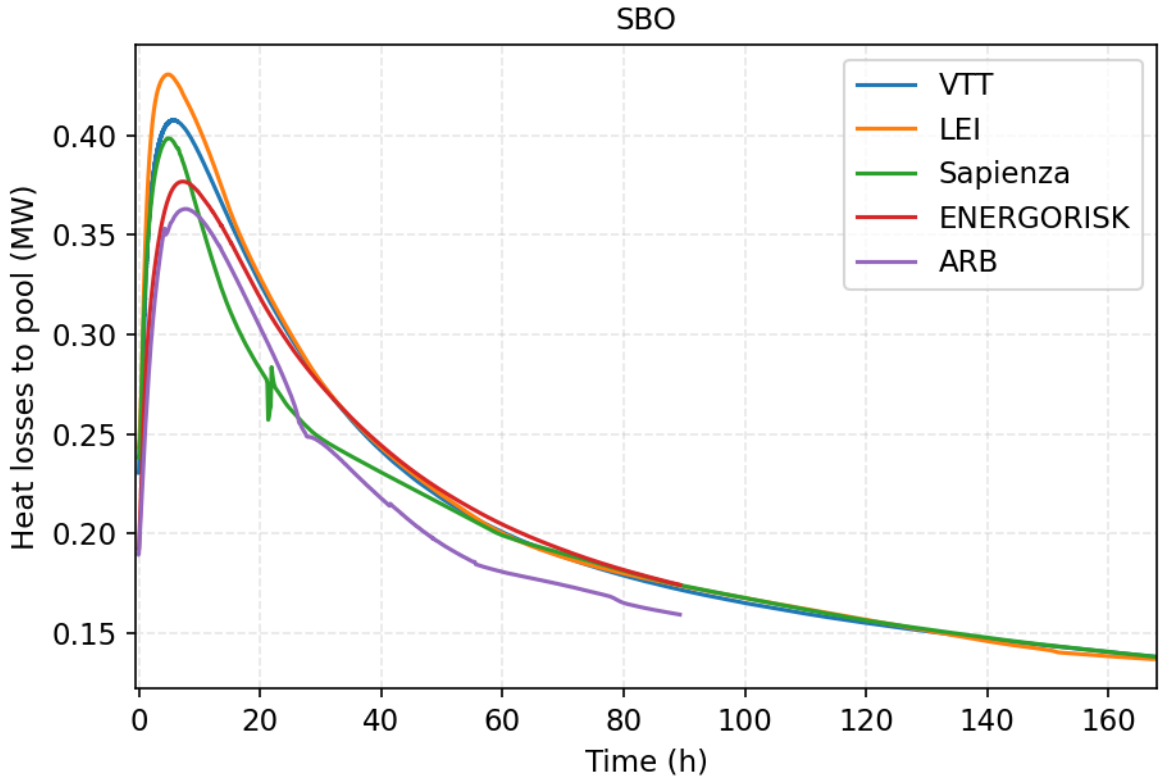

Figure 9. Heat losses to pool during SBO transient.

Co-funded by the European Union
UK Research and Innovation
The Research Council of Norway
Project funded by

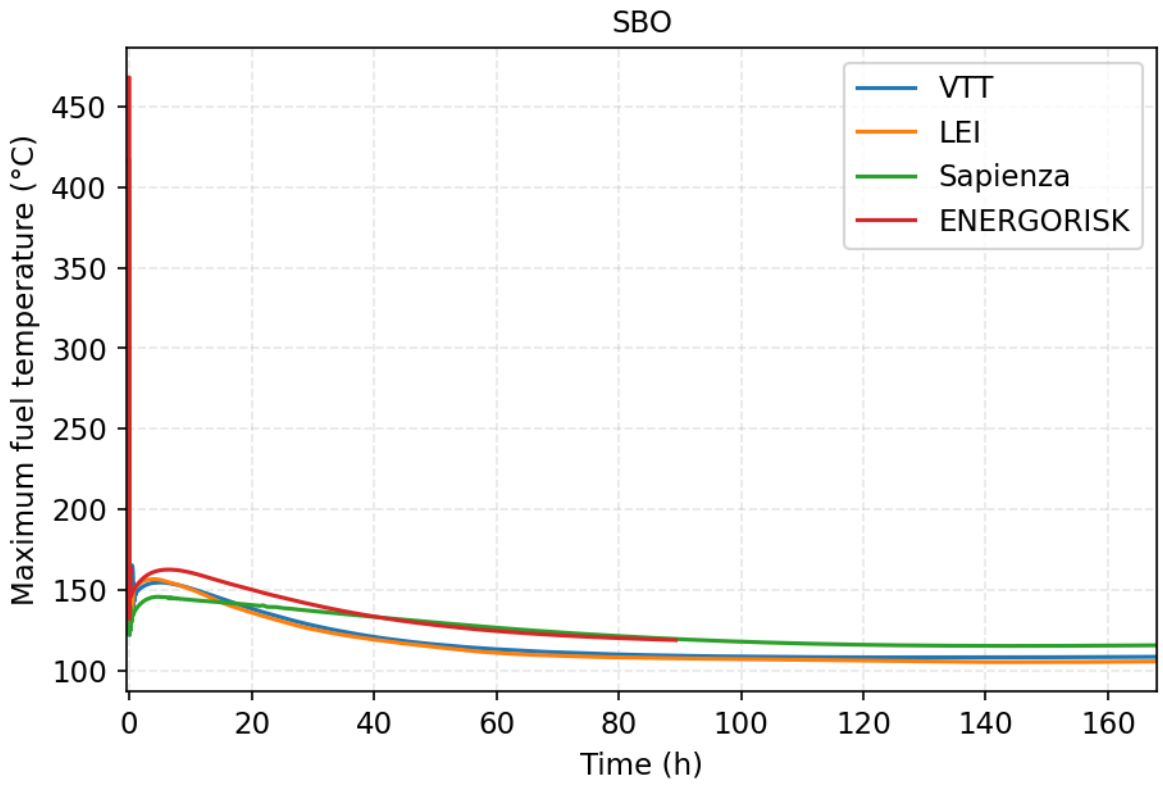

Figure 10. Maximum fuel temperature during SBO transient.

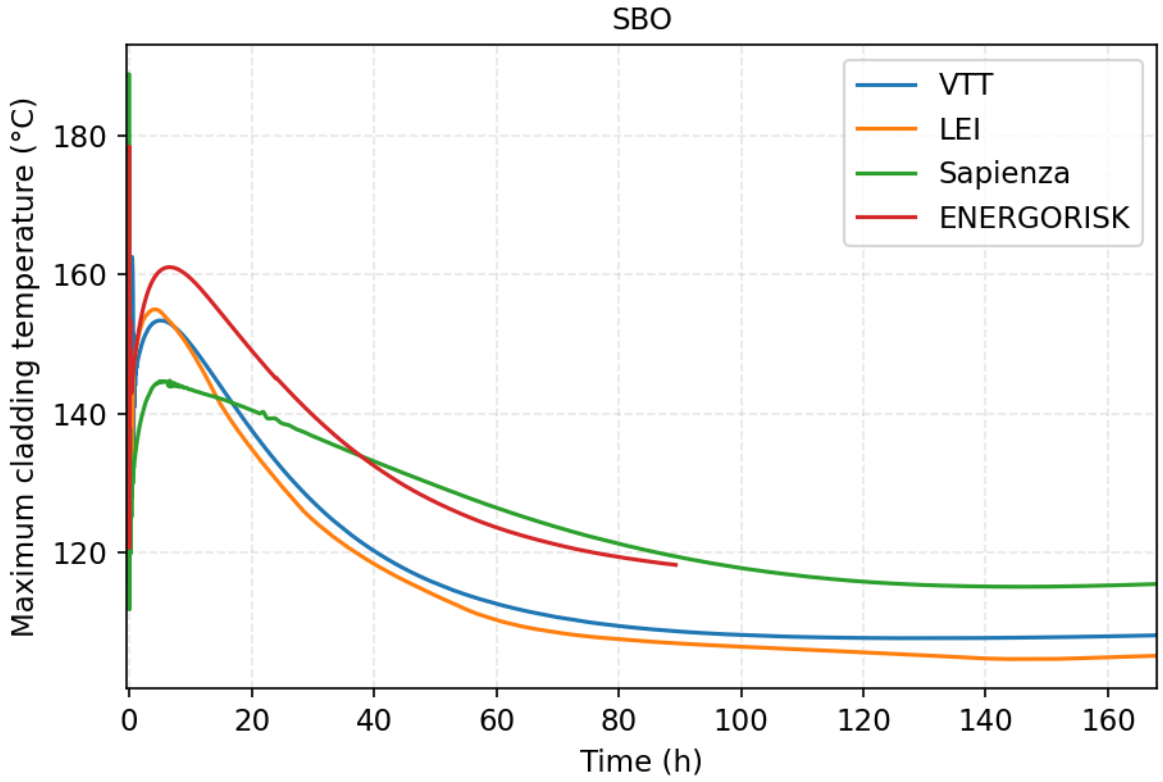

Figure 11. Maximum cladding temperature during SBO transient.

Co-funded by the European Union
UK Research and Innovation
The Research Council of Norway
Project funded by

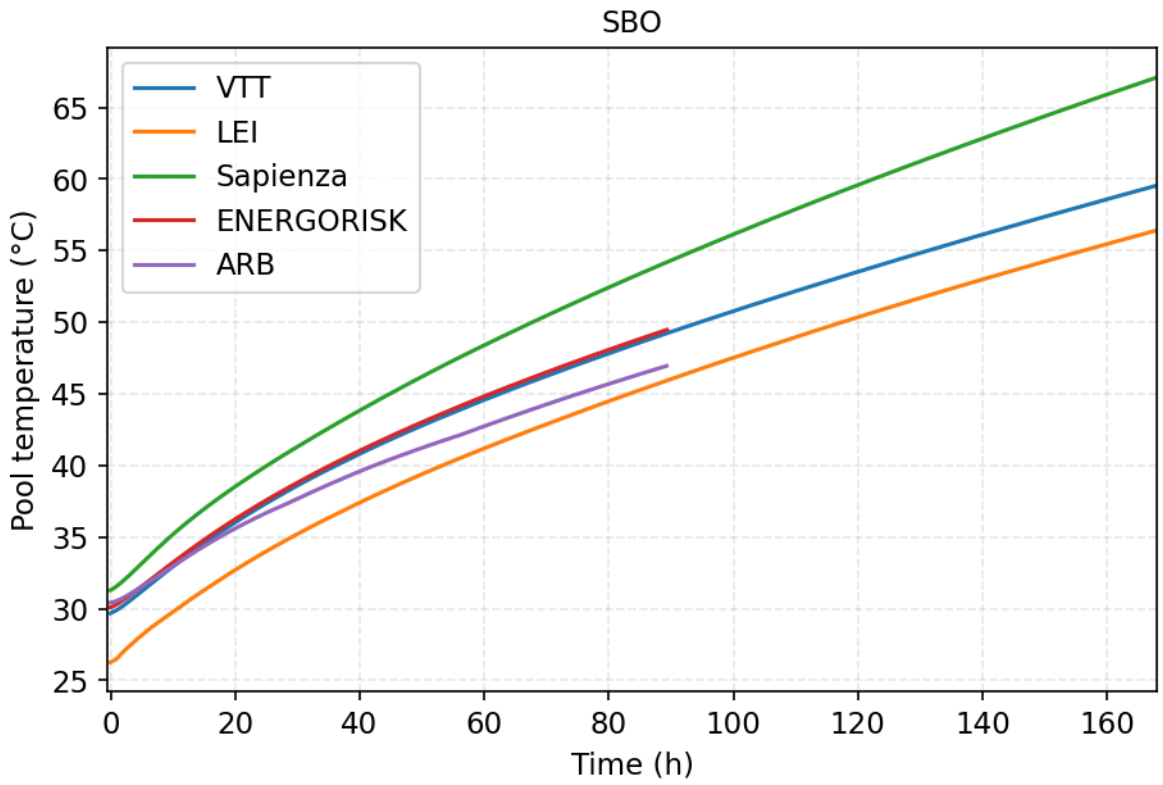

Figure 12. Pool temperature during SBO transient.

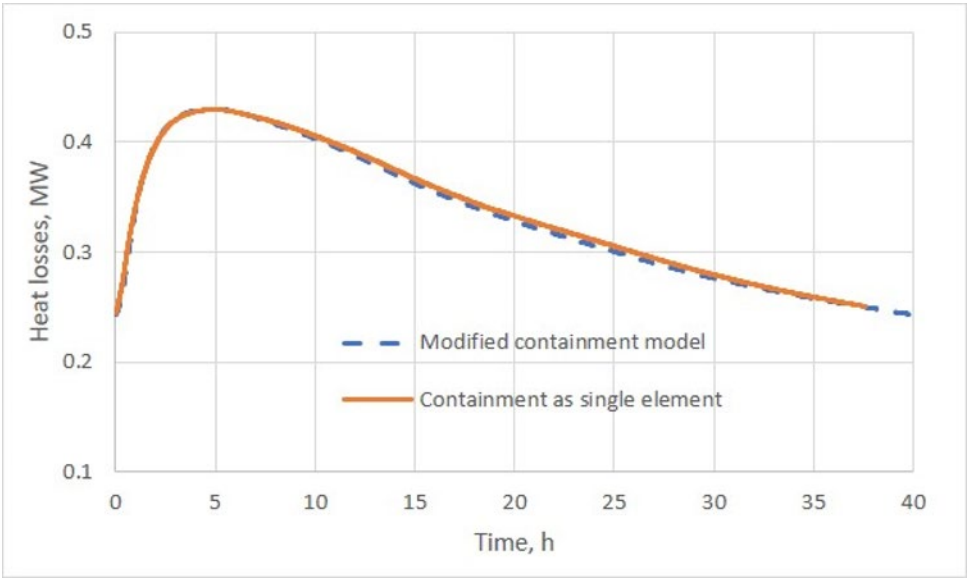

Figure 13. The heat transfer from the containment to the water pool using different containment models (LEI calculations – SBO case).

Co-funded by the European Union
UK Research and Innovation
The Research Council of Norway
Project funded by

Figure 14. The pressure behavior in pressurizer using different containment models (LEI calculations – SBO case).

10.3. SBLOCA

The results from a small break loss-of-coolant accident are presented in this section. The transient is initiated by a small break from the reactor vessel to the containment. Reactor trip is triggered by the High containment pressure signal, when the limit of 2 bars is exceeded. Energorisk used the condition to the scram signal "$dT_s \leq 10$ °C", where dT_s is the saturation temperature margin at the core outlet. The time of reactor trip from each participant is presented in Table 5. At the time of reactor trip, also the secondary circuit is isolated, after which the reactor is cooled down passively. The time of reactor trip varies between participants from 4.8 seconds to 72.1 seconds. Although the variation is large, at the time scale of the transient the differences are not significant.

Table 5. Time of reactor trip in the SBLOCA transient.

Organisation	Time of reactor trip (s)
VTT	20.65
Sapienza	4.8 (Ramson-Trapp) 7.0 (Henry-Fauske)
LEI	9.00
Energorisk	72.1*
ARB	n/a

* Energorisk used the scram signal "dTs ≤ 10 °C" - the decrease in saturation temperature margin at the core outlet. If "P_cont>2.0 bar" is used, the scram signal would be at 53.52 s.

The total break mass flow rate is presented in Figure 15. At first liquid coolant is discharged through the break (Figure 16), since the break location is below the primary water level. After the water level has decreased to the break elevation, also steam and non-condensable gases are discharged (Figure 17). The models show varying levels of gas mass flow though the break with the Energorisk model showing the highest amount,

Co-funded by the European Union
UK Research and Innovation
The Research Council of Norway
Project funded by

whereas in the VTT model the mass flow stabilizes close to zero. The total mass transferred through the break varies between models from 5.5 tons to 7.5 tons (Figure 18).

The increased steam leakage in the Energorisk (ATHLET) model can be explained by the presence of a so-called "cold" wall in the containment model due to the separation of the containment volume into ascending and descending parts (with crossflow). The "cold" wall effectively condenses the steam coming from the reactor and drains the condensate to the containment pool. This is confirmed by the increase in the water mass and level in the containment for both the ATHLET and COCOSYS models.

The influence on the simulation results of different choked flow models has been assessed by Sapienza. The SBLOCA scenario has been investigated by using both Ramson-Trapp (R-T) and Henry-Fauske (H-F) models. Results are reported in Figure 19, Figure 20 and Figure 21. Just after the Postulated Initiating Event (PIE), R-T predicts a higher mass flow with respect to H-F (blue line is above the red one in Figure 19). Instead, in the mid-term the comparison is reverted and the H-F trend lies above the R-T. When integrating the parameter, the difference in terms of mass discharged is quite reduced (see Figure 20). In the case of H-F, the primary level falls at the quote of the break (i.e., HX inlet) and the system parameters starts to show a sawtooth trend (e.g., the primary level in Figure 21). Every time primary levels drops below the break elevation, break mass flow approaches zero. Energy is introduced in the primary system due to the decay heat produced in the core. This energy causes the swelling of the primary water inventory, whose level increases again, exceeding the quote of the break and a corresponding spike of the break mass flow. This mechanism periodically repeats during the transient evolution with an increasing characteristic time (due to the gradually decreasing primary inventory). This sawtooth trend of the break mass flow and, thus, of the system parameters is absent in the case R-T choked model is adopted.

Co-funded by the European Union
UK Research and Innovation
The Research Council of Norway
Project funded by

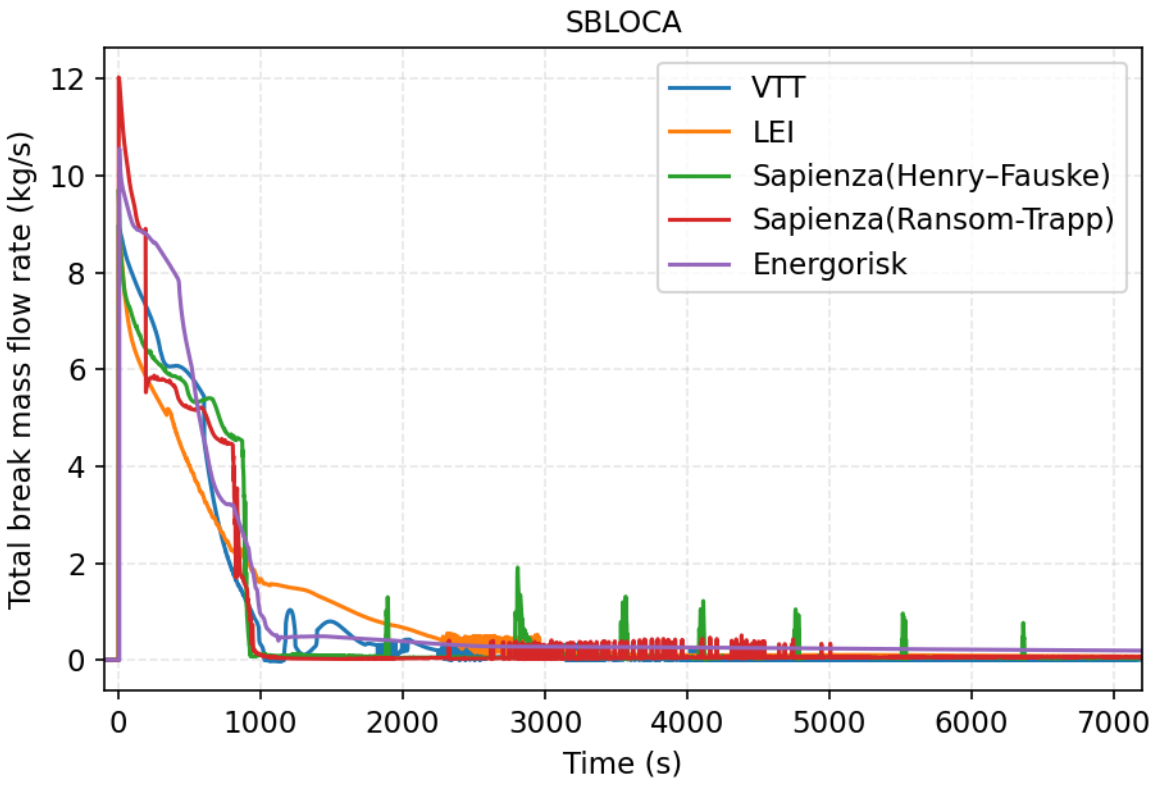

Figure 15. Total break mass flow rate during SBLOCA transient.

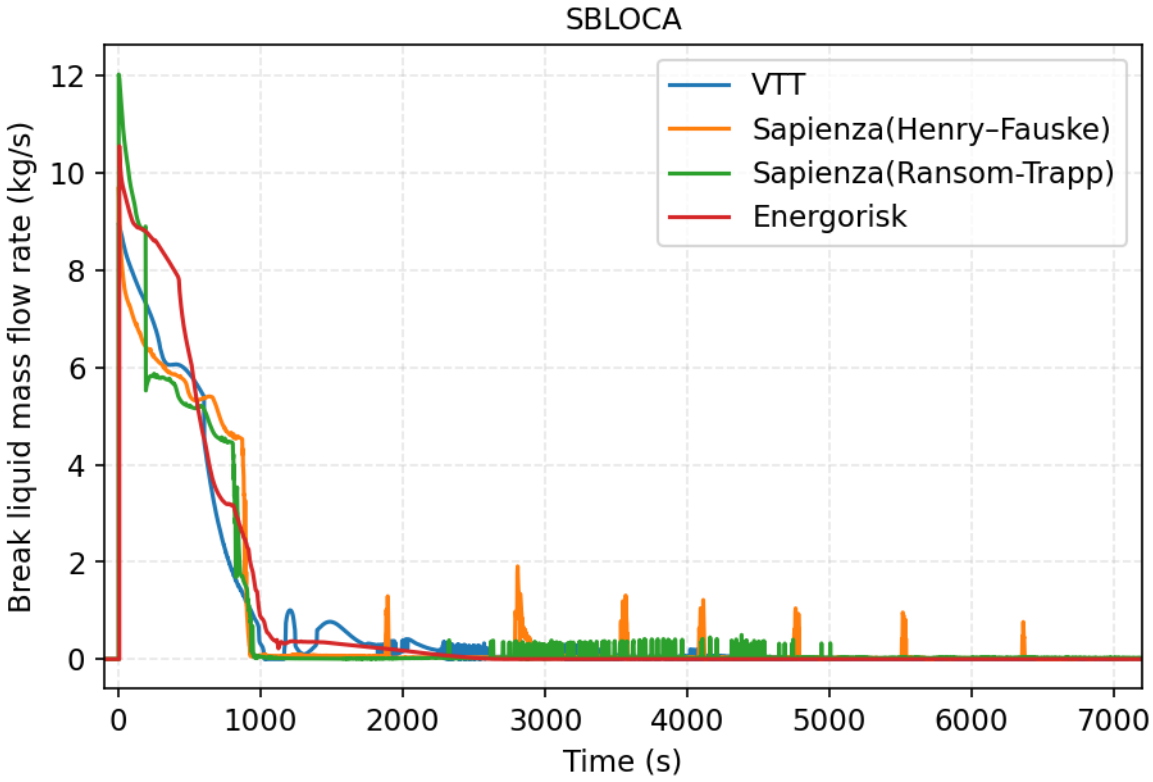

Figure 16. Break liquid mass flow rate during SBLOCA transient.

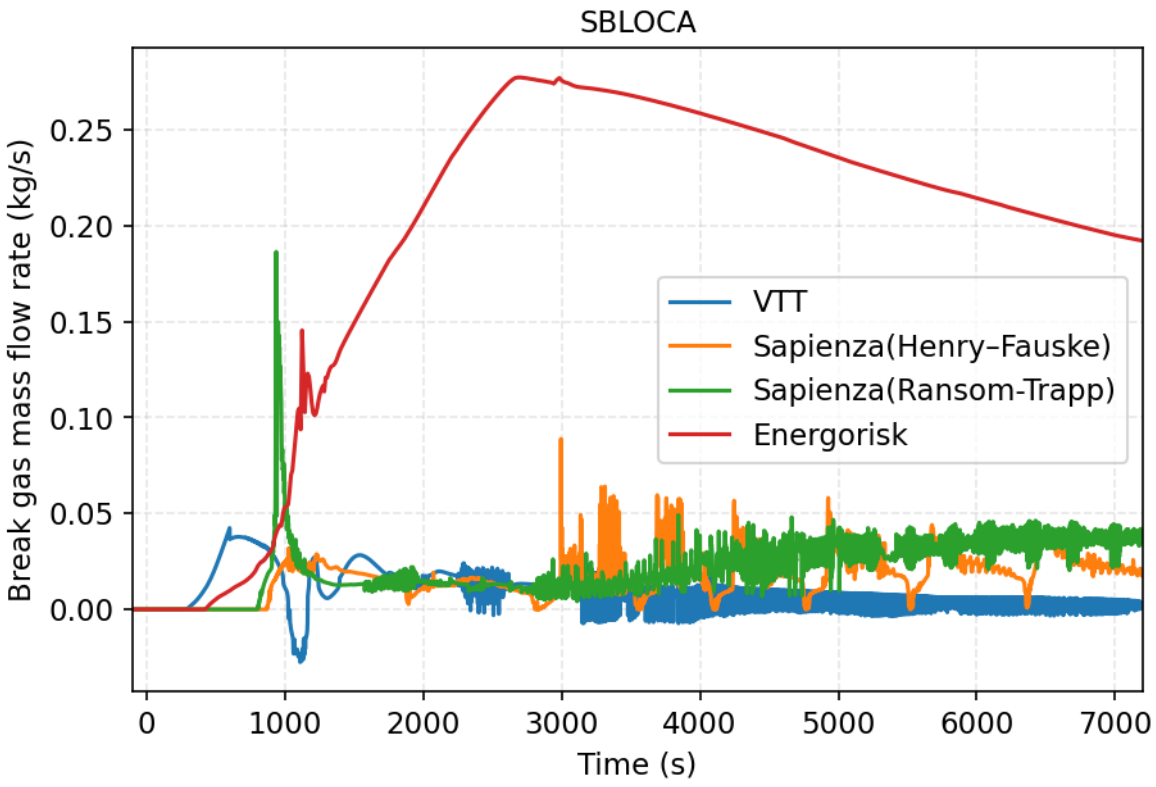

Figure 17. Break gas mass flow rate during SBLOCA transient.

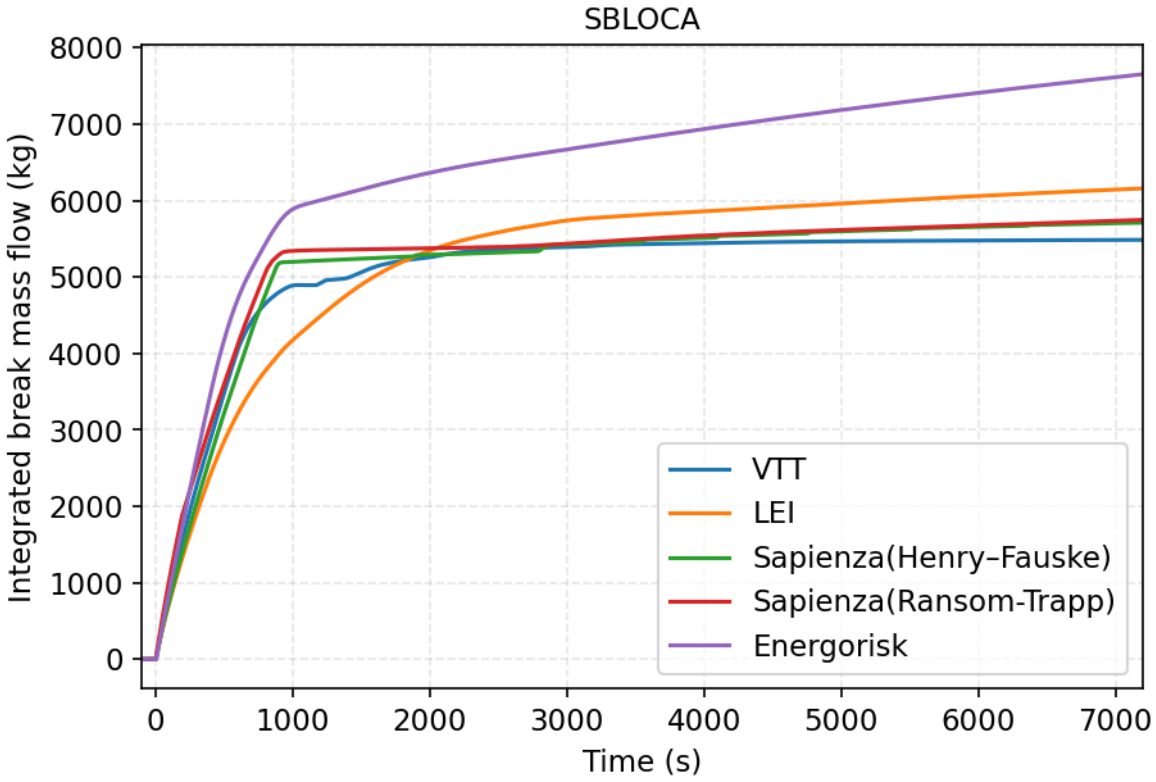

Figure 18. Integrated break mass flow during SBLOCA transient.

Co-funded by the European Union
UK Research and Innovation
The Research Council of Norway
Project funded by

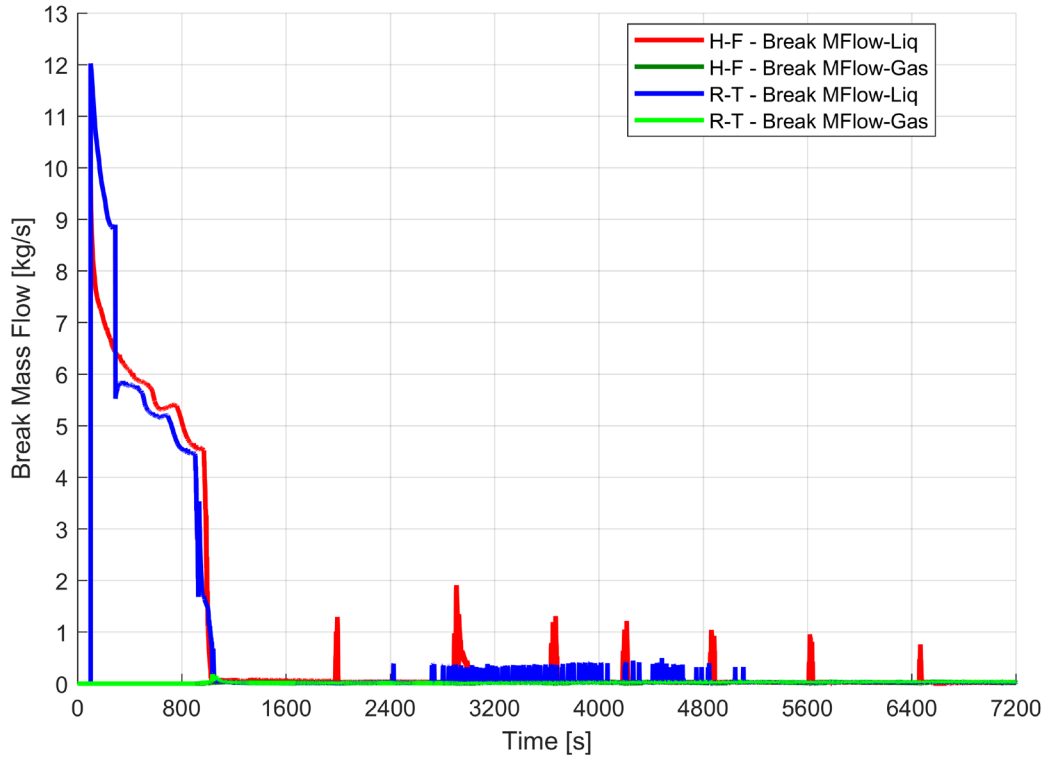

Figure 19. SBLOCA scenario: mass flow through the break predicted with Ramson-Trapp and Henry-Fauske choked flow models. For each model, both liquid and gas contributions have been plotted.

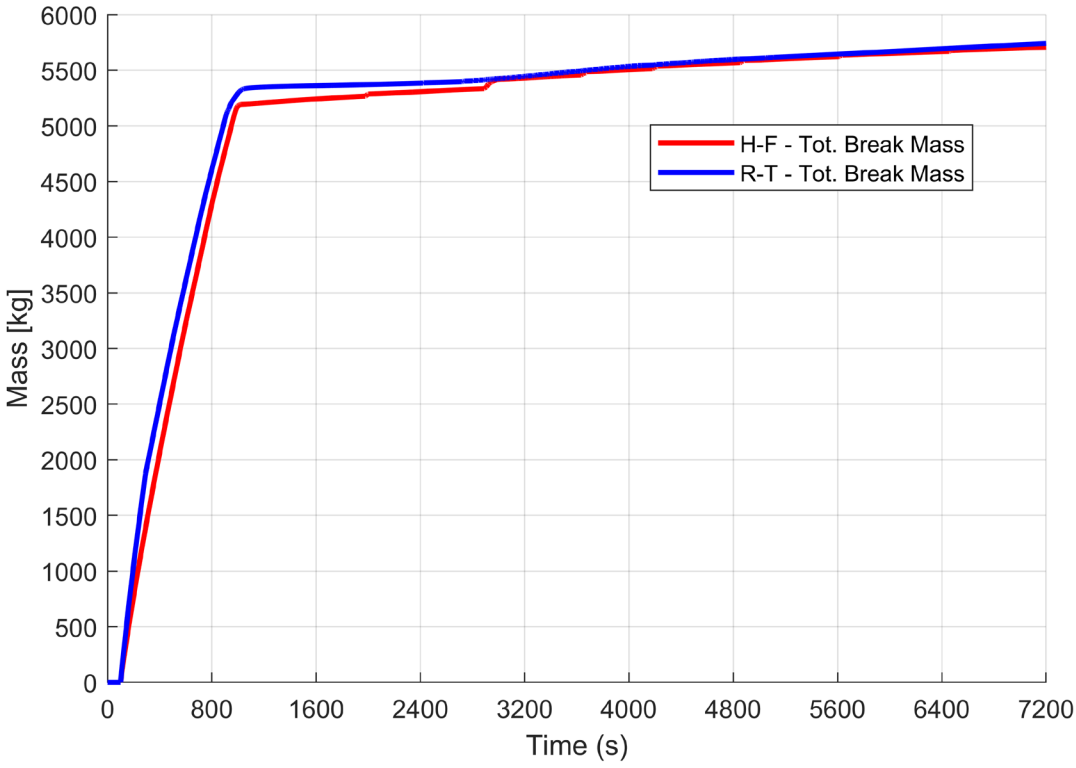

Co-funded by the European Union
UK Research and Innovation
The Research Council of Norway
Project funded by

Figure 20. SBLOCA scenario: total mass discharged through the break predicted with Ramson-Trapp and Henry-Fauske choked flow models.

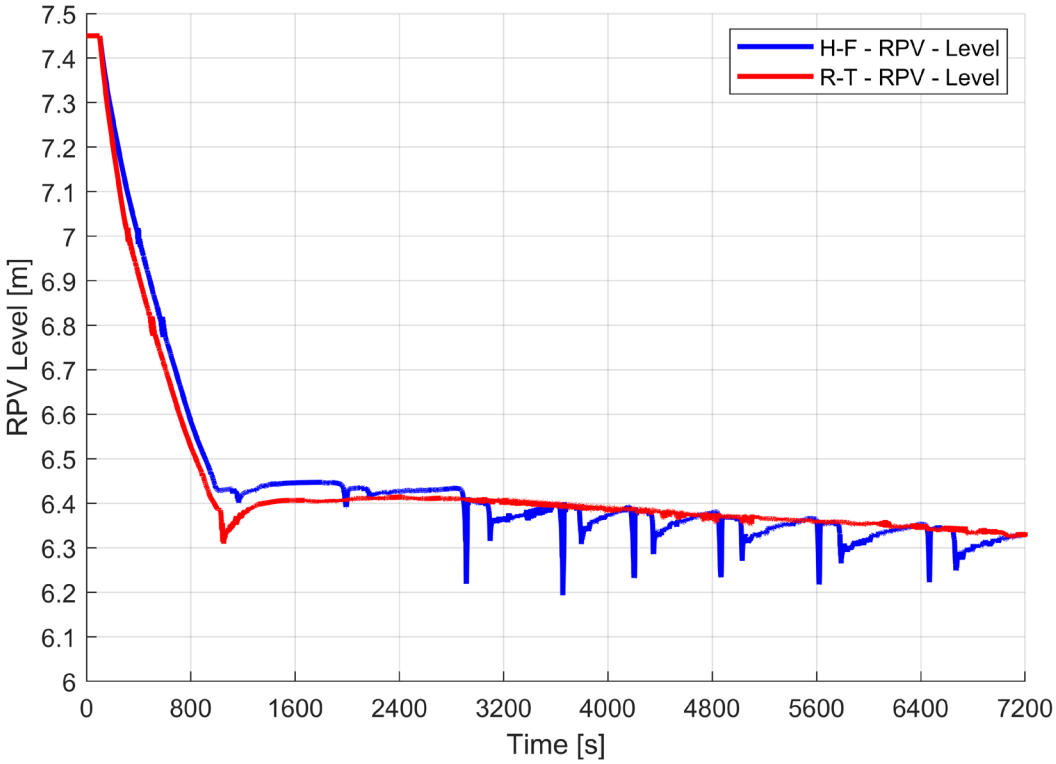

Figure 21. SBLOCA scenario: RPV collapsed level predicted by RELAP5/Mod3.3 when using Ramson-Trapp and Henry-Fauske choked flow models.

Once the primary water level (Figure 22) has decreased to break elevation and more, the natural circulation stops. This causes the coolant in the core to start boiling. However, all models show that the core remains covered with many meters of coolant on top and there are no increases in the fuel or cladding temperatures. All models also exhibit mainly positive flow through the core (Figure 23) and negative flow through the bypass (Figure 24) indicating that a smaller natural circulation loop is formed in the core. It should be noted that in reality the flow patterns would be three-dimensional in such a situation meaning that in 1D thermal-hydraulic codes the behaviour is heavily simplified.

In the ATHLET model the core is implemented using a different approach from others leading to a special behavior of coolant flows. The core contains a hot channel (hot assembly), central and peripheral channels (central and peripheral assemblies) and core bypass (guide tubes). At the steady state stage, the velocity of the coolant depends significantly on the relative amount of heat entering the channels. This explains why the velocity during steady state is highest in the hot channel and lowest in the bypass (see Figure 27). After reactor scram, the coolant movement in the core channels almost stops and then partially resumes. The decrease in the reactor level below the top of the riser (about 1000 s) does not lead to stagnation of flows in the core. The flows in the central and hot channels and the bypass keep an upward direction, while in the peripheral channel the coolant movement turns downward.

Co-funded by the European Union
UK Research and Innovation
The Research Council of Norway
Project funded by

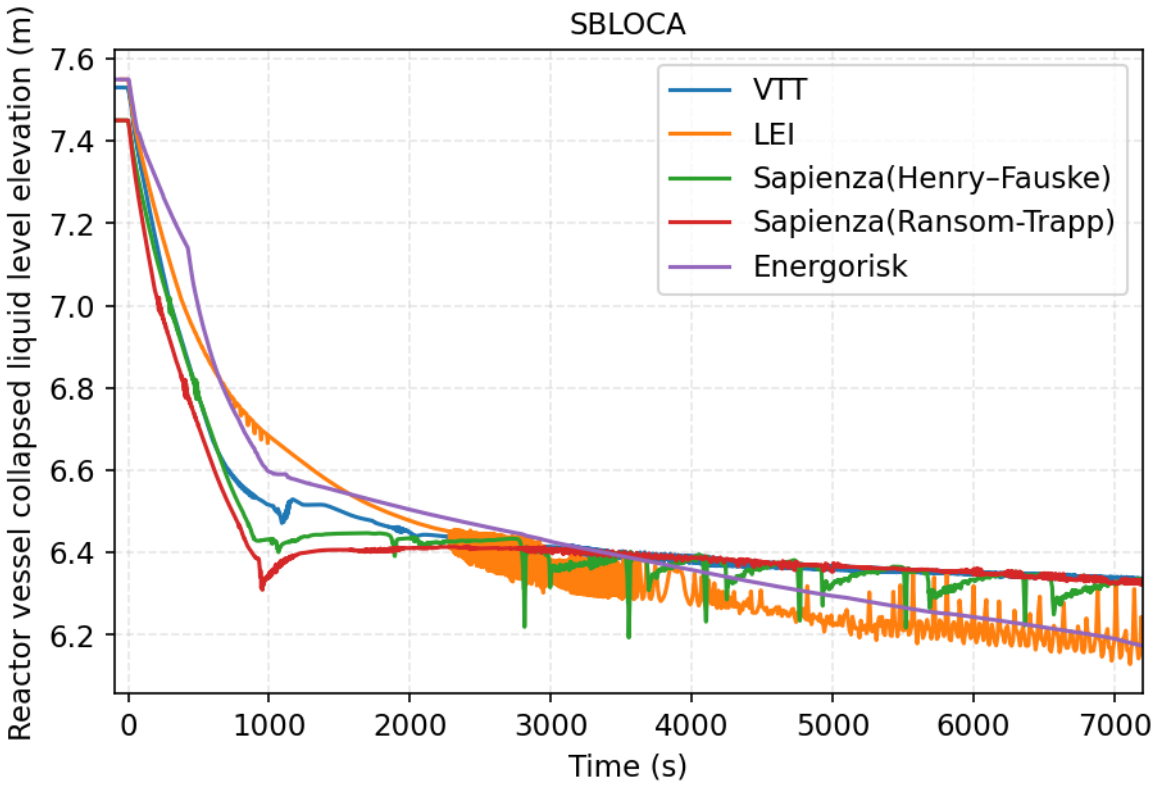

Figure 22. Reactor vessel collapsed liquid level during SBLOCA transient.

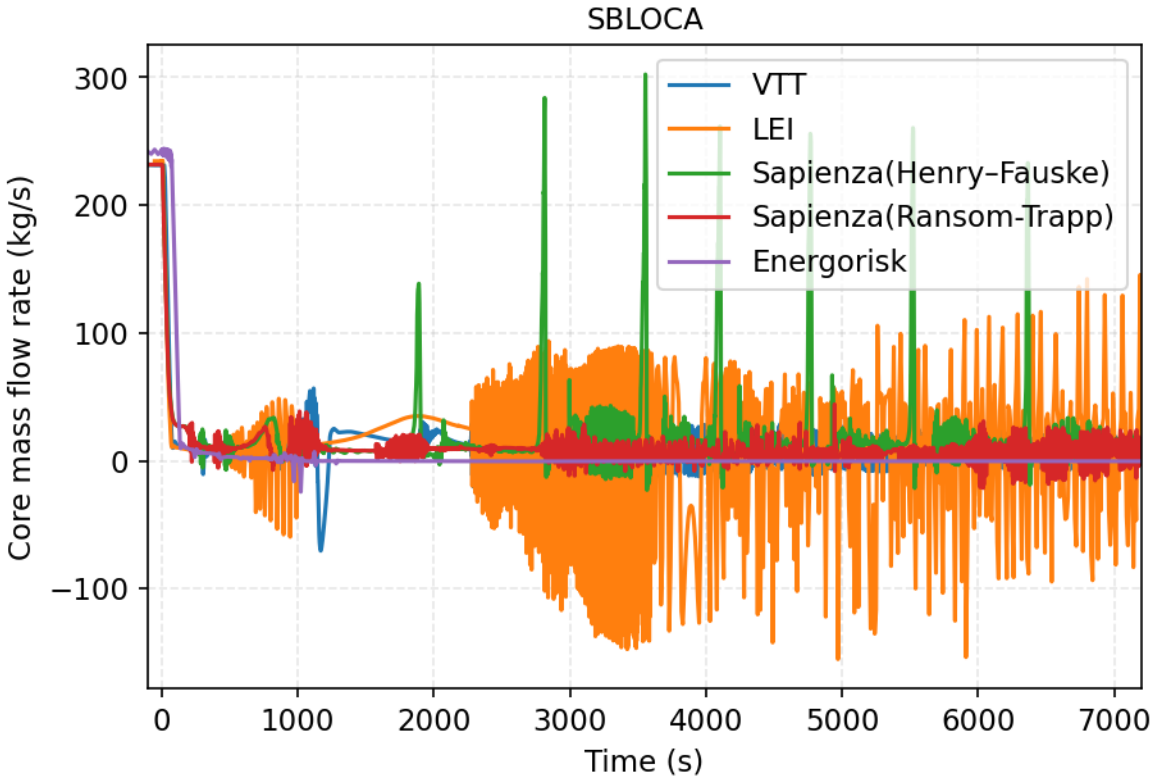

Figure 23. Core mass flow rate during SBLOCA transient.

Co-funded by the European Union
UK Research and Innovation
The Research Council of Norway
Project funded by

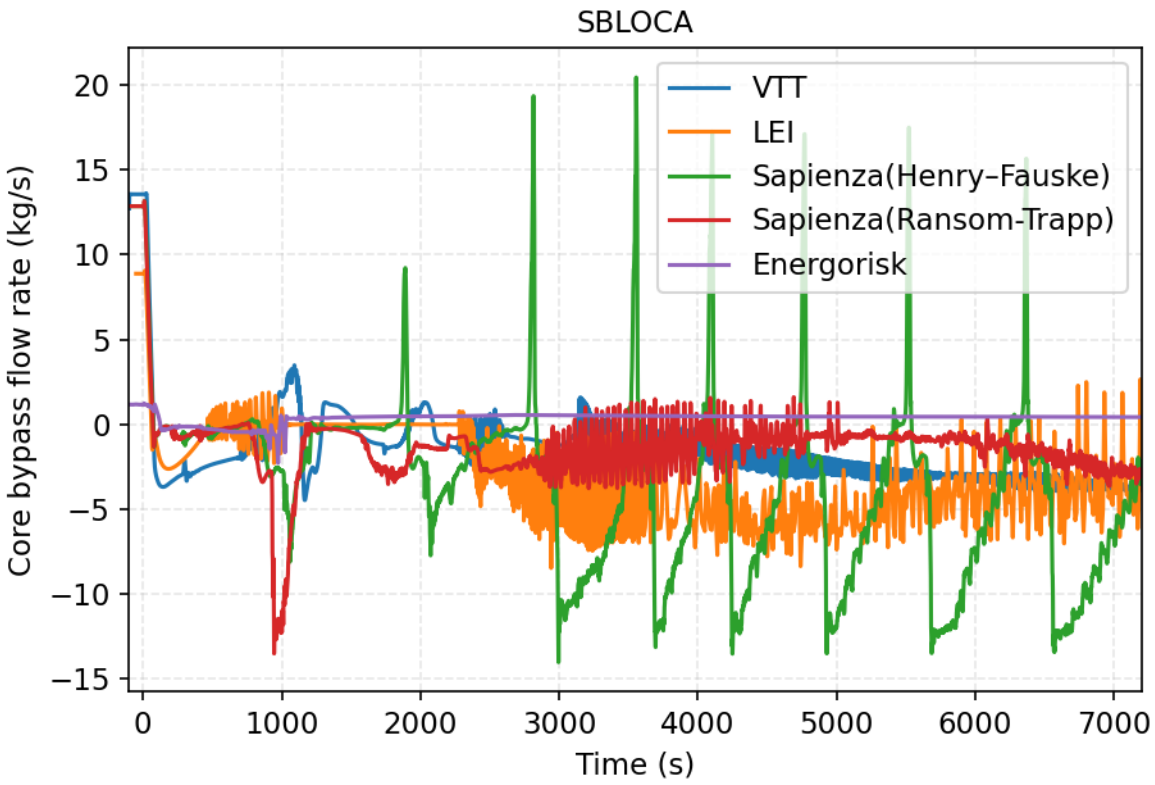

Figure 24. Core bypass mass flow rate during SBLOCA transient.

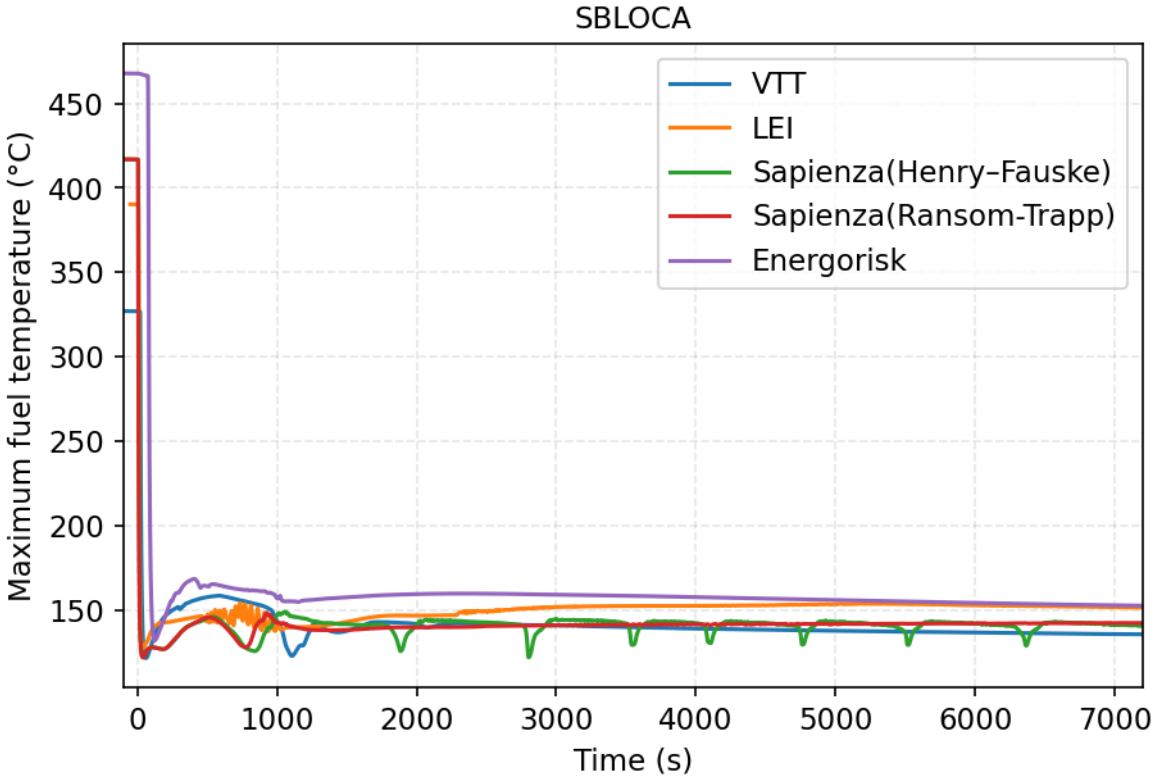

Figure 25. Maximum fuel temperature during SBLOCA transient.

Co-funded by the European Union
UK Research and Innovation
The Research Council of Norway
Project funded by

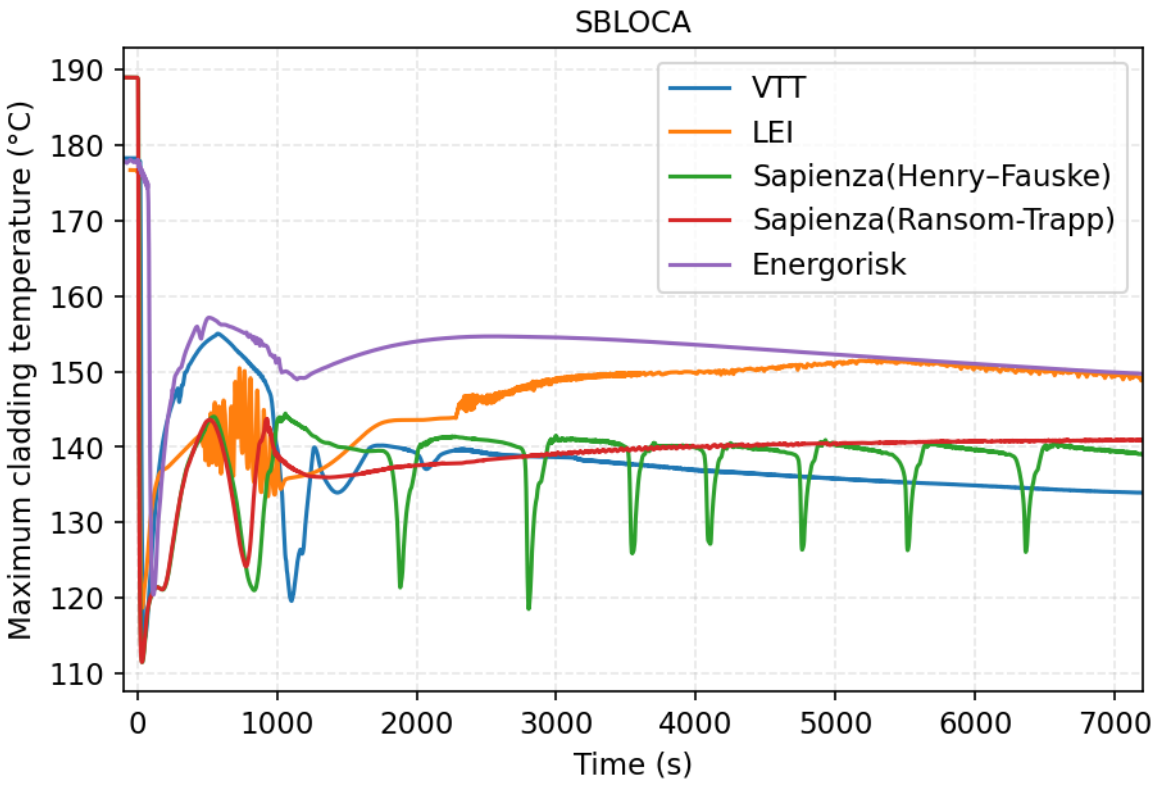

Figure 26. Maximum cladding temperature during SBLOCA transient.

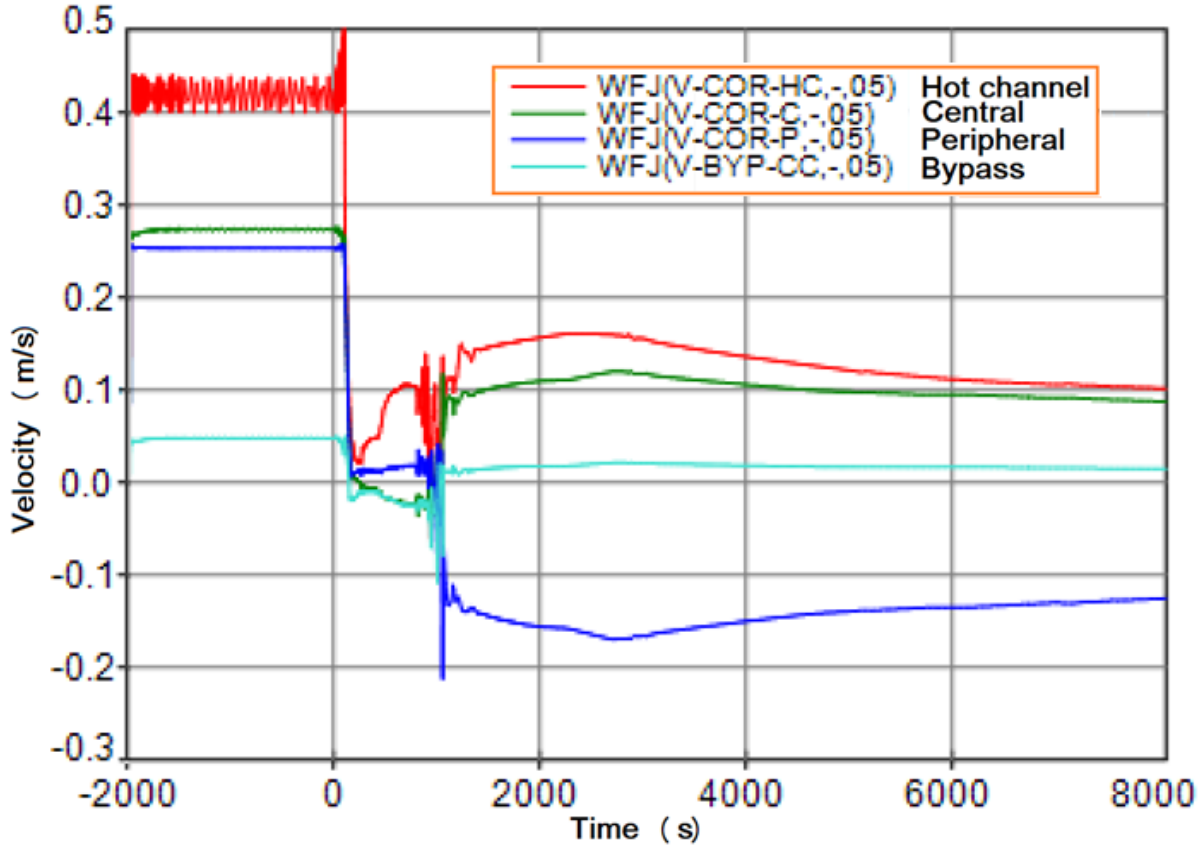

Figure 27. The SBLOCA ATHLET model velocity of the primary coolant in the reactor core channels: hot, central, peripheral, bypass.

Co-funded by the European Union
UK Research and Innovation
The Research Council of Norway
Project funded by

The primary water level keeps decreasing slowly, which is driven by the boiling in the core. The calculation would have to be continued for several hours or even days to see whether the level stabilizes at some point, however, the accuracy would suffer significantly because of accumulated mass error. If the calculation was continued further, the break mass flow would be so small that it can be the same order of magnitude as the mass error, which means that any meaningful conclusions cannot be drawn from the results.

The containment liquid level (Figure 28) increases around two meters, which enhances the heat transfer through containment to the pool significantly (Figure 29). The VTT and Energorisk models show high initial peaks in the heat transfer whereas the other models show a pattern more consistent with the increasing water level. This might suggest that the models predict some evaporation-condensation phenomenon even before the water level has increased.

The VTT and LEI models predict the highest containment pressure peak of 4 bars, whereas the other models show slightly lower pressures (Figure 30). This also affects at which level the primary pressure stabilizes (Figure 31) as pressure difference over the break evens out.

LEI performed the investigation of pressurizer nodalization influence on calculation results. The pressurizer is 1.5 m height and 7.3 m^3 volume element, placed in the reactor vessel top. In the simplified model case this pressurizer is modelled as single volume, while in the modified model – this element was divided into 3 identical volumes. The performed analysis showed, that in case of simplified model the initial (steady state) pressure in pressurizer is slightly higher than in in three volumes case (see Figure 32). This slightly higher pressure leads to slightly higher release of steam through the break within first seconds after break initiation. However, this practically do not lead to differences in containment pressure and further behaviour of pressure in pressurizer and containment remains practically identical.

Co-funded by the European Union
UK Research and Innovation
The Research Council of Norway
Project funded by

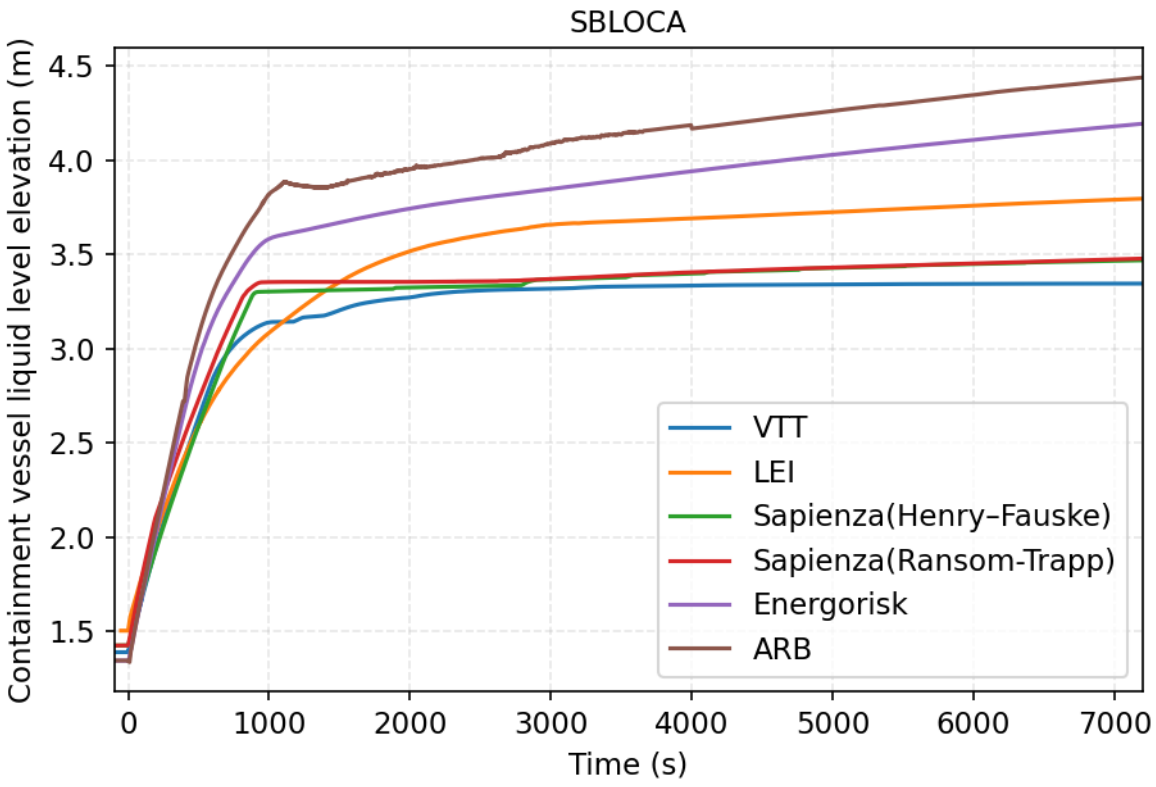

Figure 28. Containment vessel collapsed liquid level during SBLOCA transient.

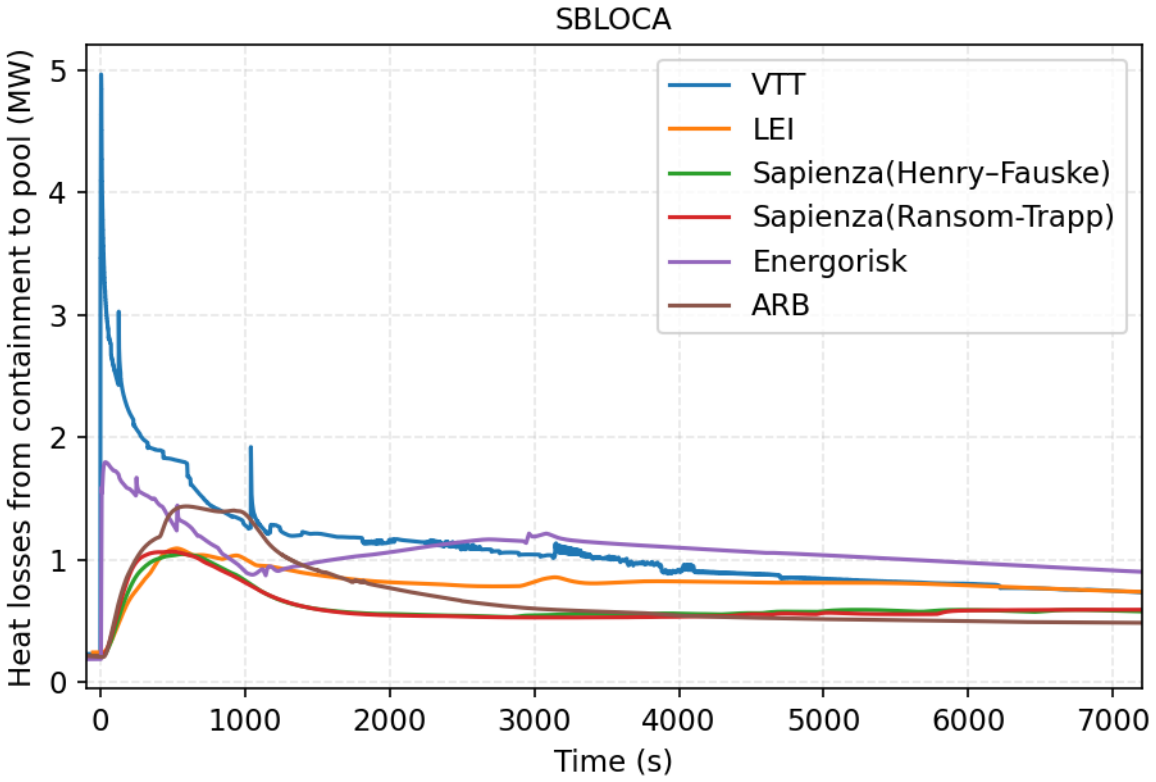

Figure 29. Heat losses from containment vessel to pool during SBLOCA transient.

Co-funded by the European Union
UK Research and Innovation
The Research Council of Norway
Project funded by

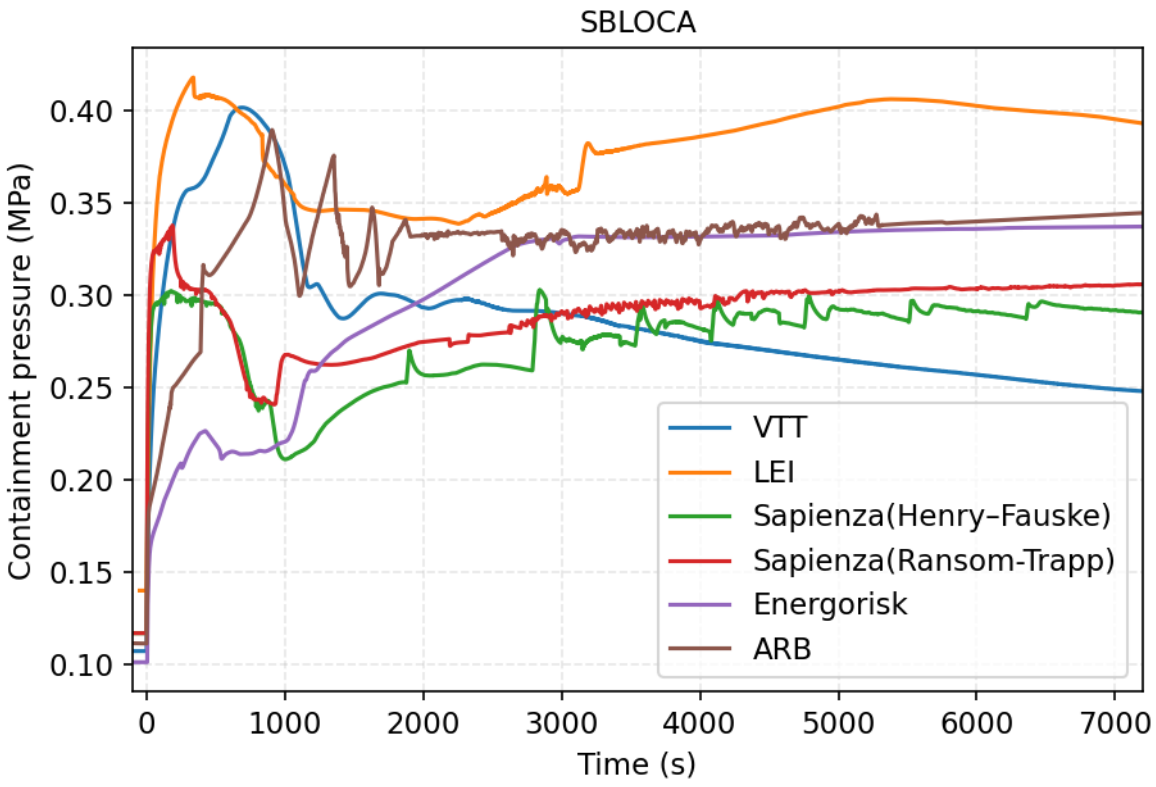

Figure 30. Containment pressure during SBLOCA transient.

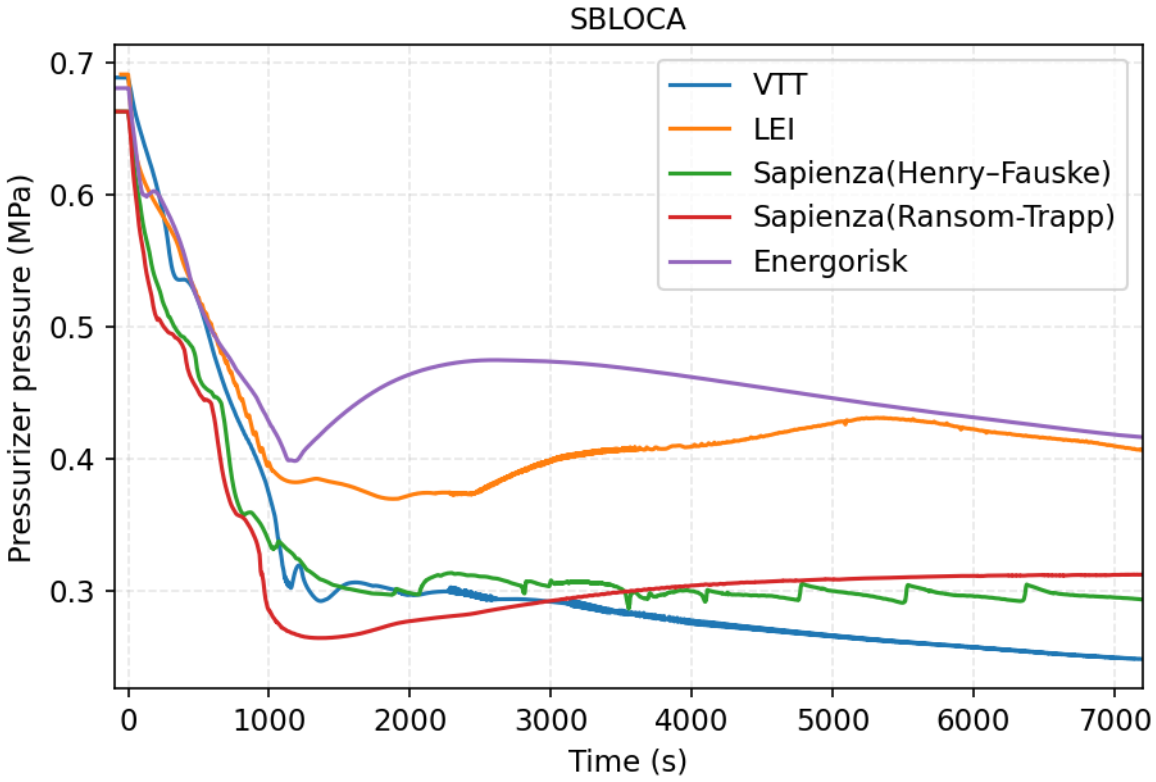

Figure 31. Pressurizer pressure during SBLOCA transient.

Co-funded by the European Union
UK Research and Innovation
The Research Council of Norway
Project funded by

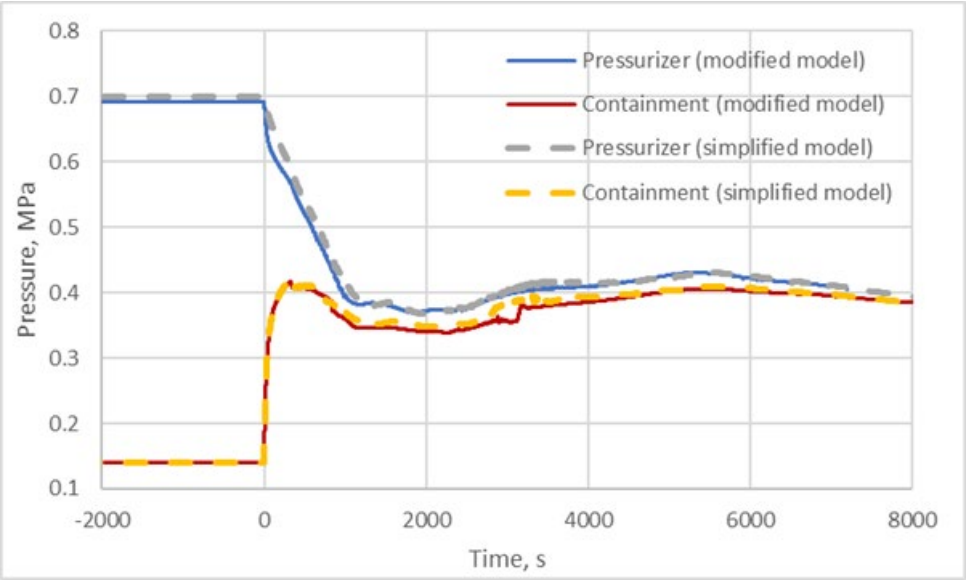

Figure 32. The pressure behaviour in pressurizer and containment using different pressurizer models (LEI calculations – SBLOCA case).

10.4. Load-follow

The results from the load-follow operation are presented in (Komu, 2026). Main results from Scenario 1 are presented in Figure 33. The reactor power follows the setpoint within the allowed one-percent tolerance limit. Power reduction is achieved by inserting the control rods, after which the xenon-135 buildup introduces negative reactivity. Further rod movement is required to compensate for the changing xenon concentration and to maintain the target power level. This results in stable oscillating behavior as the load-follow operation continues. In total the rods move within 5 cm range with a minimal impact on the axial power distribution.

The axial offset is already high in the initial state, caused by the deep insertion of control rods in the BOC conditions. The axial offset as well as the peaking factors increase slightly during the load-following. The thermal hydraulic parameters – fuel and cladding temperatures, core outlet temperature and primary pressure – stay at or below initial levels. The secondary circuit and district heating network temperatures remain constant.

In the second scenario, Figure 34, the reactor behavior is similar to the first scenario despite the irregular demand. The reactor again follows the setpoint within tolerance and the safety-relevant parameters behave similarly: slight increase in peaking factors and axial offset, while the temperatures and pressure remain at or below the initial levels. The reactor response remains stable without overshoot or instabilities. Although the power variations are large, the slow rate of change likely aids in the stable behavior supporting safe operation during load-following.

Co-funded by the European Union
UK Research and Innovation
The Research Council of Norway
Project funded by

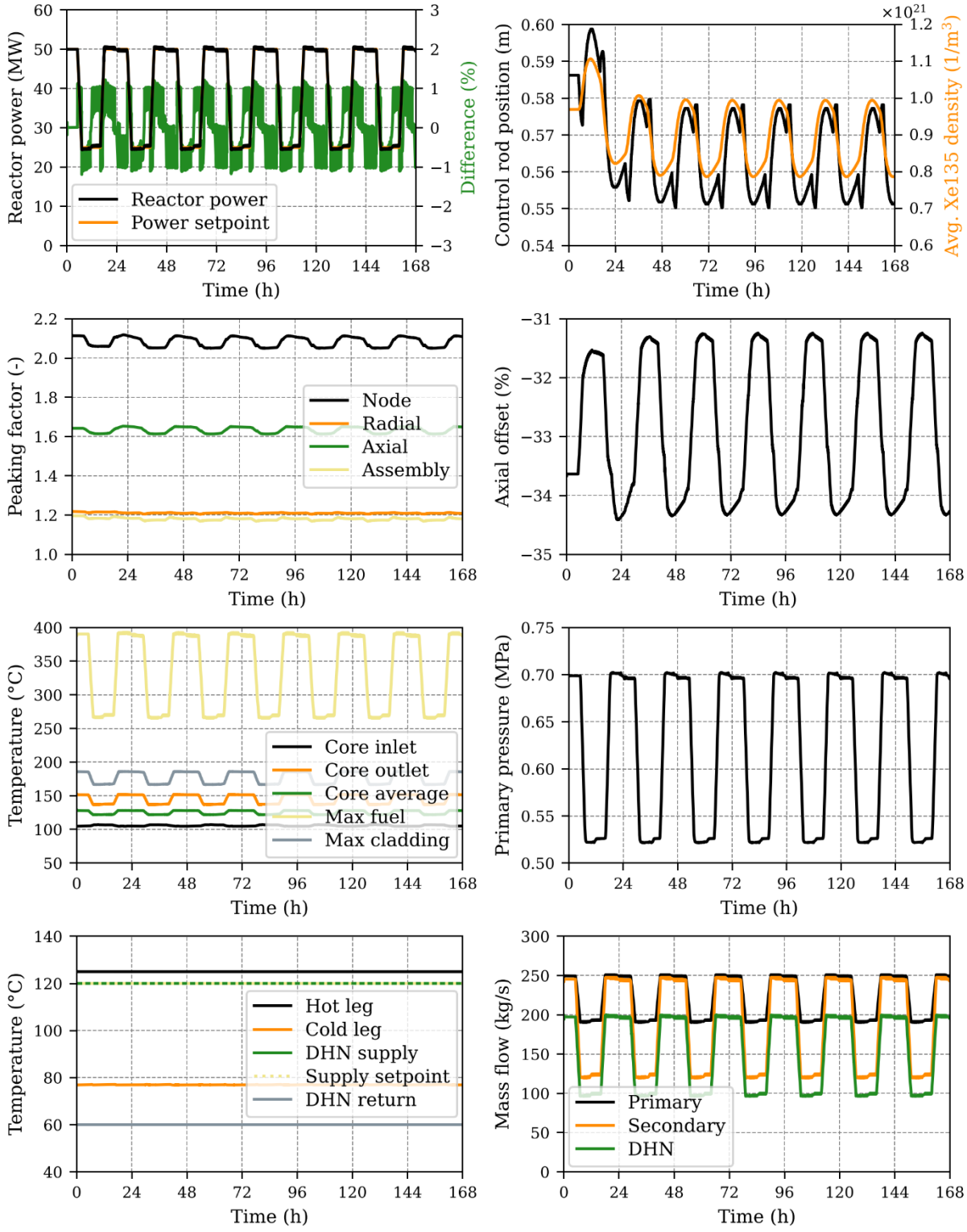

Figure 33. Results from load-follow Scenario 1 calculated with Ants-Apros (Komu, 2026).

Co-funded by the European Union
UK Research and Innovation
The Research Council of Norway
Project funded by

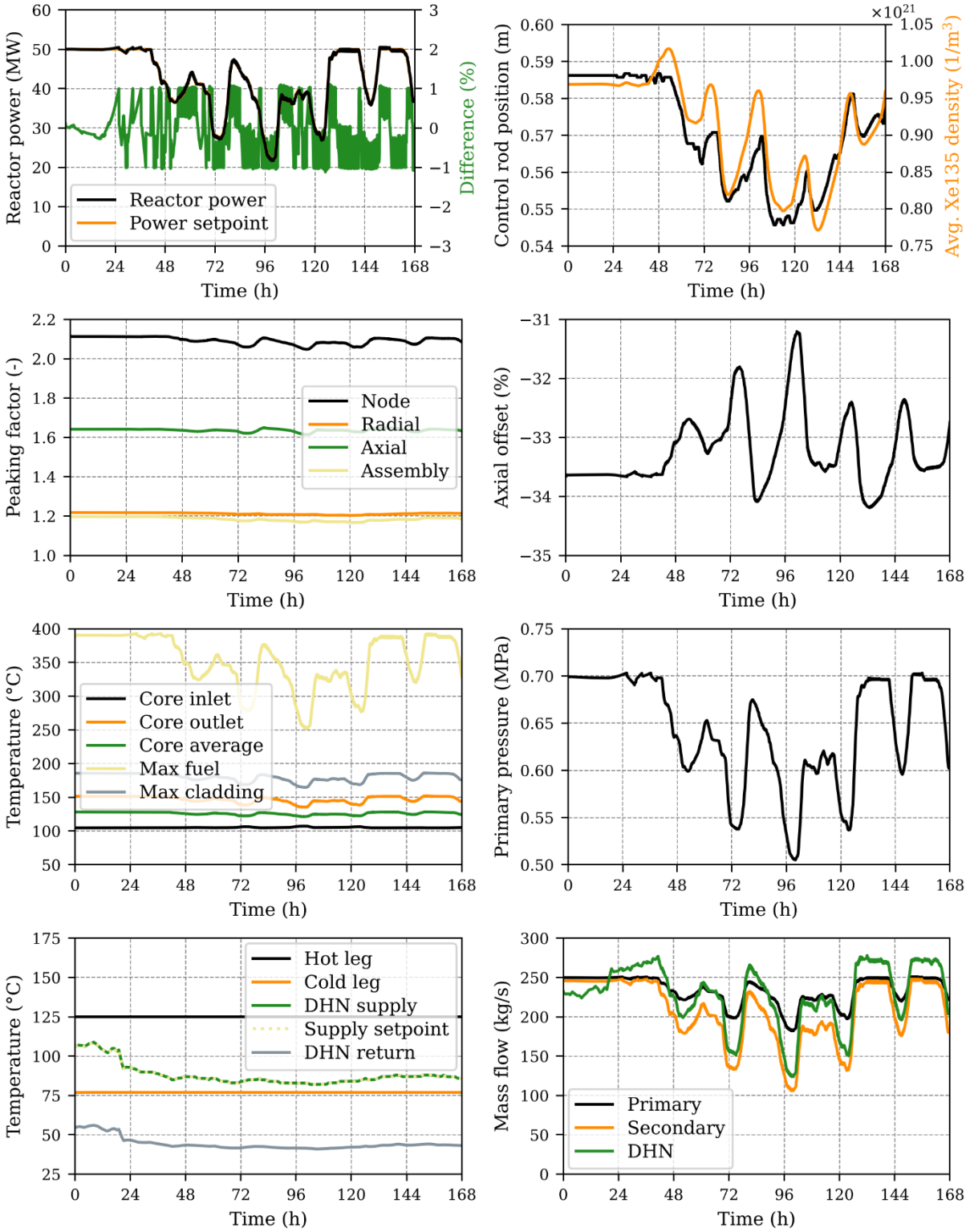

Figure 34. Results from the load-follow Scenario 2 calculated with Ants-Apros (Komu, 2026).

Co-funded by the European Union
UK Research and Innovation
The Research Council of Norway
Project funded by

11. Conclusion

This report presented a pilot study of the LDR lite district heating reactor through a code-to-code benchmark covering hot full power steady state, station blackout and small-break loss-of-coolant-accident, together with a demonstration of load-follow operation. Five organisations participated in the benchmark with system codes Apros, RELAP5, ATHLET and COCOSYS enabling a comparison of overall plant behaviour and the impact of modelling choices.

The steady-state comparison showed overall good agreement in the main thermal-hydraulic parameters, while the largest differences were related to quantities that are sensitive to nodalization and modelling differences between codes such as heat losses. In the transient analyses, all models predicted that the reactor can be cooled passively during SBO and that no cladding or fuel heat-up occurs during the simulated SBLOCA despite the loss of primary inventory and natural circulation. The code-to-code benchmark shows broadly consistent results across different system codes, while also highlighting modelling areas that benefit from further studies. Differences were seen in mass flow, pressure evolution, break discharge, and containment response demonstrating the sensitivity of results in regards of, for example, pressurizer, containment and break flow modelling. Sensitivity studies were conducted regarding the containment and pressurizer nodalization as well as chocked flow models. The load-follow analyses demonstrated stable reactor behaviour under extended heat demand variations with the main safety-relevant parameters remaining at acceptable levels.

This study provides a useful basis for further model development, deeper investigation of the remaining discrepancies, and further safety assessment of LDR lite while supporting the feasibility of passive safety systems and flexible operation.

12. Bibliography

Arndt, S., Band, S., Beck, S., Eschricht, D., Iliev, D., Nowack, H., Reinke, N., Spengler, C., Klein-Heßling, W., Sonnenkalb, M. & Weber, G. (2023). COCOSYS 3.2.0 User Manual. GRS-P-3 / Vol. 1. 2023. Cologne: Gesellschaft für Anlagen- und Reaktorsicherheit (GRS) gGmbH.

Hänninen, M. & Ylijoki, J. (2008). The one-dimensional separate two-phase flow model of APROS, VTT RESEARCH NOTES 2443, VTT Technical Research Centre of Finland.

Komu, R., Tuominen, R. & Valtavirta, V. (2025). LDR lite benchmark specifications, LDR-PUB-VTT-10002-R4, Espoo: VTT Technical Research Centre of Finland Ltd.

Komu, R. (2026). Operational Stability and Safety of LDR Lite Under Extended Load-Following Conditions. Torino, Italy, April 19 – 23, 2026, PHYSOR 2026 - The International Conference on Physics of Reactors.

NRC (2001). U. S. Nuclear regulatory commission. SCDAP/RELAP5/MOD3 code manual. User's guide and input manual. NUREG/CR-6150 3. Rev. 2 (2001).

Rintala, A. and Lauranto, U. (2023). Time-dependent neutronics model of nodal neutronics program Ants. Annals of Nuclear Energy, volume 190, p. 109868.

Schöffel, P., Di Nora, A. et al. (2024a). ATHLET 3.4.2. User's Manual. Part 2: ATHLET input data description. GRS-P-1/Vol. 1 Rev. 13. GRS.

Schöffel, P., Di Nora, A. et al. (2024b). ATHLET 3.4.2. User's Manual. GRS-P-1/Vol. 1 Rev.13. GRS.

Schöffel, P., Di Nora, A. et al. (2024c). ATHLET 3.4.2. Models and Methods. GRS-P-1/Vol. 4 Rev.10. GRS.

US Nuclear Regulatory Commission (1998). RELAP5/MOD3 Code Manual: Code Structure, System Models, and Solution Methods. NUREG/CR-5535; USNRC: Washington, DC, USA, 1998; Volume I.

Annex I. Code and model descriptions

Organization: VTT Technical Research Centre of Finland Ltd

Country: Finland

Code and version: Apros 6.14.33

PC/operative system/compiler: Windows Server 2022 Version 21H2

Description of the code:

Apros is a process simulation software developed by VTT and Fortum (Hänninen and Ylijoki, 2008). It is used for safety analysis of nuclear reactors as well as simulation of other industrial processes, conventional power plants and district heating networks. Apros includes several solvers for modelling the two-phase flow, out of which the six-equation model was used in this work.

Description of the model:

The Apros model consists of the primary circuit, containment, pool, and secondary circuit as a whole, and the district heating network with boundary conditions. 1D modelling approach is used in the primary circuit and the core is modelled with one representative channel and a bypass. The containment is modelled with one column of nodes and the pool with two in order to allow natural circulation. Heat transfer out of the pool is not modelled.

Heat structures between the riser/core and downcomer, downcomer and containment, and containment and pool model the heat transfer through the steel structures between these volumes.

The two secondary circuit loops are modelled as one. The secondary circuit mass flow rate is controlled with a pump to achieve the wanted hot leg temperature, and the same logic applies to the district heating network mass flow and outlet temperature. The inlet temperature of district heating network is given to the model as a boundary condition. Heat losses through the piping are not modelled.

Co-funded by the European Union
UK Research and Innovation
The Research Council of Norway
Project funded by

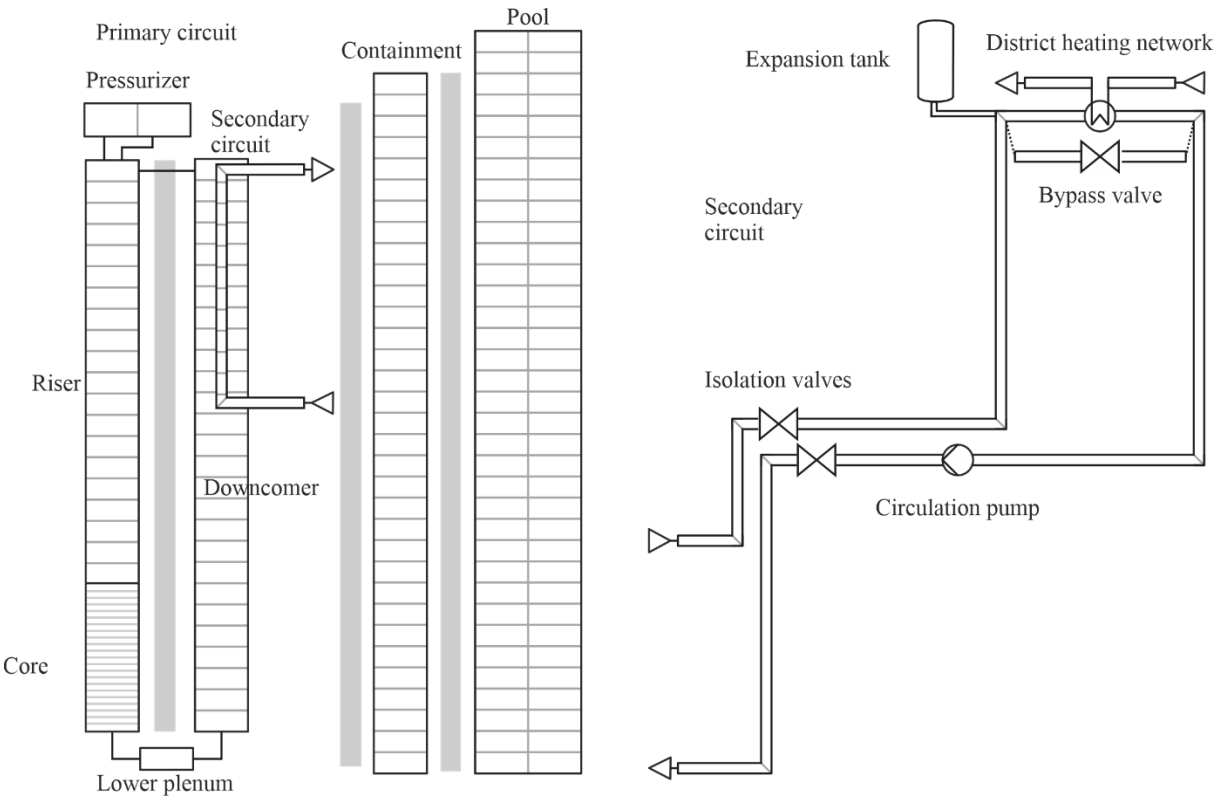

Figure 35. Schematic figure of VTT's Apros model nodalization (not in scale).

Nodalization features	
Reactor vessel nodalization (1D or 3D)	1D
Reactor vessel number of vertical flow paths / radial rings and sectors	1
Axial levels in reactor vessel	29
Core model (1D or 3D)	1D
Number of hydraulic channels in core region (radial rings and sectors)	1
Axial levels in active core	20
Axial levels in the primary heat exchanger	11
Number of secondary circuits modelled	1
Boundary conditions used in secondary circuit	pressure
District heating circuit modelled?	Yes
Total number of TH nodes in containment	66
Axial levels in containment	33
Total number of TH nodes in the pool	70
Axial levels in pool	35
Code options	
Choked flow model applied (e.g. Ramson-Trapp, Henry Fauske, etc.)	Moody + stagnation pressure
Specific models activated in PRZ (YES or NO and specify the model)	No

Co-funded by the European Union
UK Research and Innovation
The Research Council of Norway
Project funded by

Specific models activated in containment (YES or NO and specify the model)	No
CCFL model (if activated, specify where in the primary system)	No
Dissolved nitrogen model (YES or NO and specify the model)	No

Parameter	Unit	Calculated
Hydraulic volumes		
Total primary circuit	m^3	40.963
Total secondary circuit	m^3	27.253
Containment	m^3	29.848
Pool	m^3	1508.045
Elevations		
Primary circuit		
Reactor vessel bottom (inside of RPV)	m	-0.63
Core active region bottom (BAF)	m	0.1175
Core active region top (TAF)	m	1.1175
PRZ top (inside RPV)	m	8.51997
HX inlet (active region)	m	6.44
HX outlet (active region)	m	3.64
Secondary circuit		
HX inlet (active region)	m	3.64
HX outlet (active region)	m	6.44
Containment		
Containment bottom	m	-0.96
Containment top	m	8.84997
Pool		
Pool bottom	m	-0.96

Organization: LEI Lithuanian Energy Institute

Country: Lithuania

Code and version: RELAP5/Mod3

PC/operative system/compiler: Windows

Description of the code:

The RELAP5 code has been developed by Idaho National Engineering Laboratory (NRC, 2001) for best estimate transient simulation of light water reactor during design basis accidents. The code models coupled behaviour of the reactor coolant system and the core for loss-of-coolant accidents, and operational transients. The hydrodynamic model of RELAP5 is a one-dimensional, non-homogeneous, non-equilibrium two-fluid model, which is solved by fast, partially implicit numerical scheme. The basic field equations for the two-phase system consist of mass, momentum, and energy relations for each of the phases. The presence of boron and noncondensable gases is also modelled using separate equations for each. Constitutive models represent the interphase drag, the various flow regimes in vertical and horizontal flow, wall friction, and interphase mass transfer.

RELAP5 code in Lithuanian Energy Institute (LEI) is used since 1995.

Description of the model:

For the analysis of thermal-hydraulic processes in LDR Lite reactor, the model for RELAP5 code is developed (Figure 36):

- The reactor core was simplified and only thermal-hydraulic (no reactor neutronics) was modelled. The reactor core is modelled by four flow paths (max, min, average power and core bypass).
- The secondary circuit is modelled only with boundary conditions.
- Heat transfer from bottom and top in axial direction from the reactor vessel into containment are not modelled.
- Containment is modelled using two identical vertical pipe elements with crosflows. This allows to model the heat transfer in the gap between reactor vessel and containment vessel – the heat could be transferred using convection of coolant.
- Water pool is modelled using two identical vertical pipe elements with crosflows.
- The containment and water pool are modelled as a group of concentric cylindrical rings.
- In the RELAP5 model the outside walls of water pool are not modelled (adiabatic condition is assumed).

Co-funded by the European Union
UK Research and Innovation
The Research Council of Norway
Project funded by

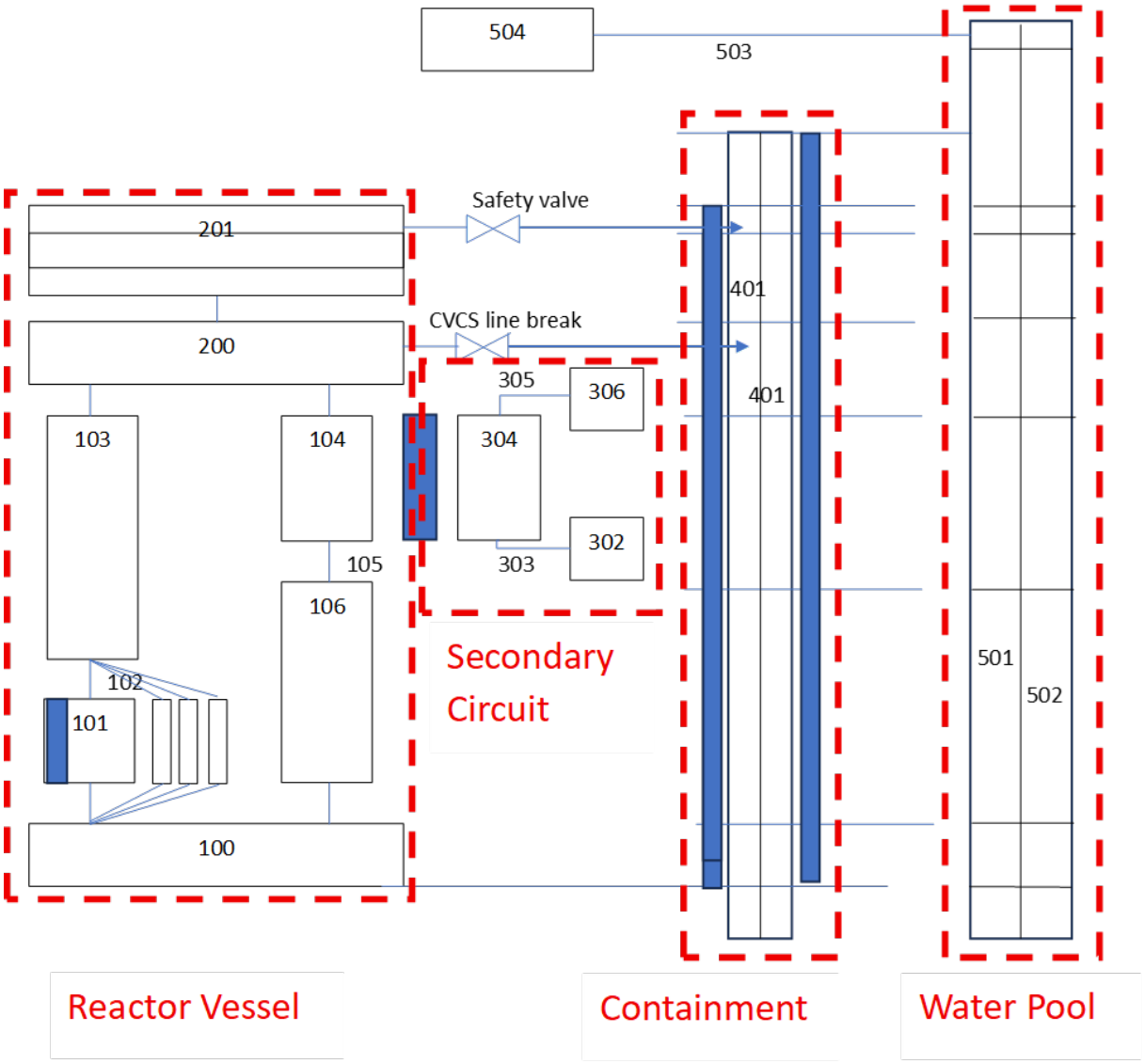

Figure 36. LDR Lite reactor model nodalisation scheme, developed for RELAP5 code.

The volume of primary circuit in the reactor vessel is ~ 41 m^3. The volume of containment is ~ 27.5 m^3, while the water mass is ~ 5000 kg. The water pool volume is 1000 m^3 (mass is 10E+05 kg) (Komu, et al., 2025). Initially, at cold state (at zero reactor power) the pressure in pressurizer and containment is atmospheric, water temperature in reactor and containment is 20°C. The water level in pressurizer is 7.02 m, and containment water level – 1.7 m, when the bottom of reactor lower plenum is at elevation 0.0 m.

Nodalization features	
Reactor vessel nodalization (1D or 3D)	1D
Reactor vessel number of vertical flow paths / radial rings and sectors	2 (risser + downcomer)
Axial levels in reactor vessel	11 axial levels from lower plenum to pressurizer
Core model (1D or 3D)	1D
Number of hydraulic channels in core region (radial rings and sectors)	3 core paths + core by-pass
Axial levels in active core	8 levels in active core + 2 unheated levels
Axial levels in the primary heat exchanger	4
Number of secondary circuits modelled	1
Boundary conditions used in secondary circuit	Pressure & temperature at inlet / outlet
District heating circuit modelled?	No
Total number of TH nodes in containment	2 flow paths
Axial levels in containment	14
Total number of TH nodes in the pool	2 flow paths
Axial levels in pool	16
Code options	
Choked flow model applied (e.g. Ramson-Trapp, Henry Fauske, etc.)	Henry Fauske
Specific models activated in PRZ (YES or NO and specify the model)	NO
Specific models activated in containment (YES or NO and specify the model)	NO
CCFL model (if activated, specify where in the primary system)	NO
Dissolved nitrogen model (YES or NO and specify the model)	NO

Parameter	Unit	Calculated
Hydraulic volumes		
Total primary circuit	m^3	40.88
Total secondary circuit	m^3	NA
Containment	m^3	27.5
Pool	m^3	1133
Elevations		
Primary circuit		
Reactor vessel bottom (inside of RPV)	m	-0.63

Core active region bottom (BAF)	m	0.1773
Core active region top (TAF)	m	1.1773
PRZ top (inside RPV)	m	8.52
HX inlet (active region)	m	6.44
HX outlet (active region)	m	3.64
Secondary circuit		
HX inlet (active region)	m	3.64
HX outlet (active region)	m	6.44
Containment		
Containment bottom	m	-0.96
Containment top	m	8.85
Pool		
Pool bottom	m	-0.96

Co-funded by the European Union
UK Research and Innovation
The Research Council of Norway
Project funded by

Organization: Sapienza University of Rome

Country: Italy

Code and version: RELAP5/Mod3.3

PC/operative system/compiler: Windows 10 Pro Version 22H2

Description of the code:

The RELAP5/Mod3.3 code (US Nuclear Regulatory Commission, 1998) is based on a nonhomogeneous and nonequilibrium model for the two-phase system that is solved by a fast, partially implicit numerical scheme to permit economical calculation of system transients. The RELAP5 development effort was aimed at producing a code that included important first-order effects necessary for accurate prediction of system transients but that was sufficiently simple and cost effective so that parametric or sensitivity studies can be carried out.

The code includes many generic component models from which general systems can be simulated, including pumps, valves, pipes, heat releasing or absorbing structures, reactor kinetics, electric heaters, jet pumps, turbines, compressors, separators, annuli, pressurizers, feedwater heaters, ECC mixers, accumulators, and control system components. In addition, special process models are included for effects such as form loss, flow at an abrupt area change, branching, choked flow, boron tracking, and noncondensable gas transport.

The hydrodynamic model and the associated numerical scheme are based on the use of fluid control volumes and junctions to represent the spatial character of the flow. The control volumes can be viewed as stream tubes having inlet and outlet junctions. The control volume has a direction associated with it that is positive from the inlet to the outlet. Velocities are located at the junctions and are associated with mass and energy flow between control volumes. Control volumes are connected in series, using junctions to represent a flow path. All internal flow paths, such as recirculation flows, must be explicitly modelled in this way since only single liquid and vapor velocities are represented at a junction. (In other words, a counter-current liquid-liquid flow cannot be represented by a single-junction.)

Heat flow paths are also modelled in a one-dimensional sense, using a finite difference mesh to calculate temperatures and heat flux vectors. The heat conductors can be connected to hydrodynamic volumes to simulate a heat flow path normal to the fluid flow path. The heat conductor or heat structure is thermally connected to the hydrodynamic volume through a heat flux that is calculated using heat transfer correlations. Electrical or nuclear heating of the heat structure can also be modelled as either a surface heat flux or as a volumetric heat source. The heat structures are used to simulate pipe walls, heater elements, nuclear fuel pins, and heat exchanger surfaces.

Description of the model:

The RELAP5/Mod3.3 (R5) model developed to simulate the transient behavior of LDR-50 reactor is shown in Figure 37.

Co-funded by the European Union
UK Research and Innovation
The Research Council of Norway
Project funded by

The reactor core is simulated following the assembly-by-assembly approach. A R5 pipe component is associated with each Fuel Assembly (FA, 37 pipes, #201-237 in Figure 37). This has been done since benchmark specifications provide the power data differentiated for each FA. Benchmark specifications also give a detailed axial power profile. The same axial mesh has been adopted in the current R5 model (the average mesh length is of 5 cm). In addition, the core bypass has been modelled with a dedicated pipe component (#12). To sum up, the core region has been simulated with 38 parallel pipes. Instead, two single volumes components have been used for the lower support plate (#10) and the upper support plate (#13). The core power is given in input to the model as boundary condition, considering all the data indicated in the benchmark specifications and mentioned above. Neutronics is not considered and the input deck accounts only for thermal-hydraulic effects.

The riser is represented by a vertical pipe (#20) with an average vertical mesh length of 20 cm. The Upper Plenum (UP) component, just below the pressurizer, has been modelled with two vertical stacks of three branches (#30, 32 and 34 for the central riser region and #31, 33 and 35 for the external annular downcomer region). The two stacks share the same axial nodalization. Mesh lenght is of nearly 20 cm for all the mentioned branches. The DownComer (DC) annulus is split in two vertical sections. The upper one coincides with the Heat eXchanger (HX) region. The vertical discretization in the DC region reflects the one belonging to the riser region. DC is finally connected to the Lower Plenum (LP), simulated by a vertical pipe of three Control Volumes (CV) of 21 cm. Above the UP, there is the pressurizer (PRZ), simulated with a vertical pipe of 15 components (average mesh length of 10 cm).

The two secondary loops have been collapsed in an equivalent one, where flow areas and mass flows have been doubled. Instaed, pipeline lengths and hydraulic diameters have been kept (respecting the rules of the hydraulic equivalence). The secondary system has been completely modelled, including the District Heating Heat Exchangers. However, this part of the input has not been included in Figure 37 and will not be extensively described in this section since not relevant for the current simulation activity.

The containment has been represented by a stack of vertical components, one above the other, whose vertical discretization reflects the one of the RPV. The adoption of multiple pipes is to make easier the writing of the thermal components. In the lower region, two multiple pipes have been adopted to properly simulate the natural convection occurring within the water volume.

Instead, the external pool has been simulated by three parallel vertical pipes. Each one accounts for one third of the water inventory (i.e., 1000/3=333.3 m^3). Multiple junction components have been used to laterally connect the corresponding volumes belonging to the same axial slice. The central channel is the one used to thermally couple the containment with the pool to simulate the heat losses from the former to the latter.

Summarizing, the 'Slice Nodalization Technique' has been used for all the input deck. This means that a vertical segmentation of the overall system to be modelled, i.e., LDR-50 reactor, has been performed on the basis of reference selected quotes. These quotes have been chosen to keep the actual design elevations. The axial mesh related to all the system components (riser, core, DC, HX, PRZ, containment, external pool) has been

obtained respecting these reference fixed heights. As a result, the same mesh length (or submultiple) was used for the vertical control volumes belonging to different nodalization regions positioned at the same axial level. This technique improves the capability of the code to reproduce natural circulation. When adopted, fluid properties are evaluated at the same axial elevations for all the nodalization regions, resulting in a proper evaluation of the natural circulation driving force and avoiding an error source on the simulation outcomes.

For what concerns the thermal model, R5 Heat Structure (HS) components have been used for:

- Simulate the fuel pins belonging to the core active region. Power terms have been entered in the input deck differentiated FA per FA and considering the axial power profile provided by the benchmark specifications.
- Simulate the primary-to-secondary heat transfer through the HX tubes.
- Simulate the heat transfer from riser to DC region thorugh the barrel.
- Simulate the system heat losses, i.e., the convective/conductive heat transfer problem through RPV and Containment walls. Instead, the outside walls of the external water pool have not been modelled and an adiabatic boundary condition has been associated with this component.

The mentioned thermal objects allow also to account for the huge steel inventory present in the LDR-50 reactor.

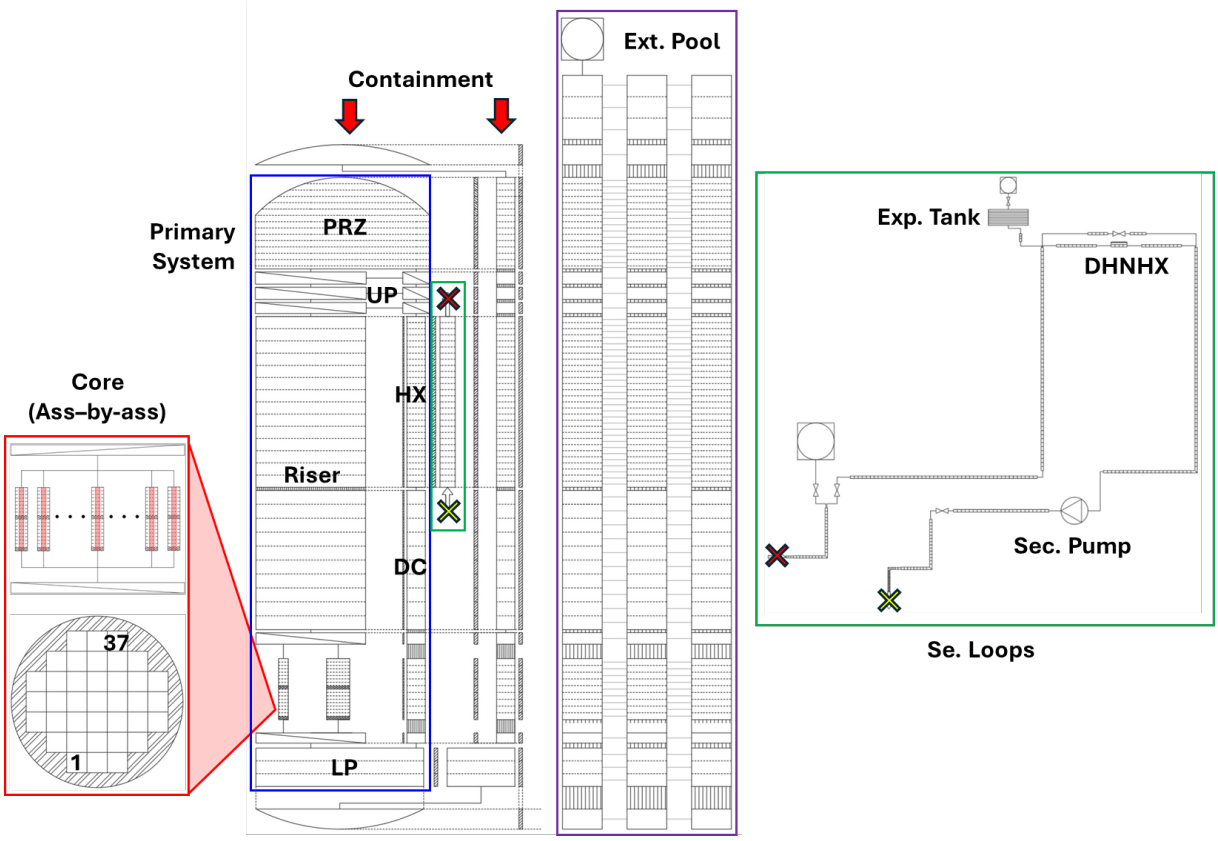

Figure 37. LDR-50 nodalization scheme developed by Sapienza with RELAP5/Mod3.3 (not in scale).

Nodalization features	
Reactor vessel nodalization (1D or 3D)	1D
Reactor vessel number of vertical flow paths / radial rings and sectors	2, one for the riser and one for the downcomer
Axial levels in reactor vessel	65 (from LP bottom to PRZ top)
Core model (1D or 3D)	1D
Number of hydraulic channels in core region (radial rings and sectors)	38, 37 FAs (assembly-by-assembly approach) + core bypass
Axial levels in active core	18 (as for benchmark specifications)
Axial levels in the primary heat exchanger	28
Number of secondary circuits modelled	The 2 secondary loops were collapsed in 1 equivalent
Boundary conditions used in secondary circuit	No BCs used, secondary loop completely modelled
District heating circuit modelled?	yes
Total number of TH nodes in containment	

Co-funded by the European Union
UK Research and Innovation
The Research Council of Norway
Project funded by

Axial levels in containment	72 axial levels from containment bottom to top
Total number of TH nodes in the pool	216 (three parallel vertical pipes)
Axial levels in pool	72 axial levels from pool bottom to top
Code options	
Choked flow model applied (e.g. Ramson-Trapp, Henry Fauske, etc.)	Both Ramson-Trapp and Henry Fauske models have been considered
Specific models activated in PRZ (YES or NO and specify the model)	NO
Specific models activated in containment (YES or NO and specify the model)	NO
CCFL model (if activated, specify where in the primary system)	NO
Dissolved nitrogen model (YES or NO and specify the model)	NO

Parameter	**Unit**	**Calculated**
Hydraulic volumes		
Total primary circuit	m^3	40.86
Total secondary circuit	m^3	19.38
Containment	m^3	29.85
Pool	m^3	1000
Elevations		
Primary circuit		
Reactor vessel bottom (inside of RPV)	m	-0.63
Core active region bottom (BAF)	m	0.1675
Core active region top (TAF)	m	1.1675
PRZ top (inside RPV)	m	8.52
HX inlet (active region)	m	6.44
HX outlet (active region)	m	3.64
Secondary circuit		
HX inlet (active region)	m	3.64
HX outlet (active region)	m	6.44
Containment		
Containment bottom	m	-0.96
Containment top	m	8.85
Pool		
Pool bottom	m	-0.96
The reference quote is assumed coincident with the bottom of the Lower Support Plate.		

Organization: Energorisk Ltd

Country: Ukraine

Code and version: AC^2 2023-3

PC/operative system/compiler: Windows 10

Description of the code:

The thermal-hydraulic computer code ATHLET (Analysis of THermal-hydraulics of LEaks and Transients) is being developed by the Gesellschaft für Anlagen und Reaktorsicherheit (GRS) (Schöffel et al., 2024a).

ATHLET is an advanced best-estimate system code which has been initially developed for the analysis of operational conditions, abnormal transients and all kinds of leaks and breaks (including design basis and beyond design basis accidents) in nuclear power plants for PWRs, BWRs, SMRs and future Gen IV reactors.

The one-dimensional, two-phase fluid dynamic models are based on a five-equation model supplemented by a full-range drift-flux model, including a dynamic mixture-level tracking capability. Moreover, a two-fluid model based on six conservation equations is provided. The heat conduction and heat transfer module allows a flexible simulation of fuel rods and structures. Nuclear heat generation is calculated by a point-kinetics model or with a coupled 3D neutron kinetics code. A general control simulation module is provided for flexible modelling of BOP and auxiliary plant systems.

Description of the model:

Thermal hydraulics objects of the LDR-50 ATHLET model are simulated taking into account the requirements, recommendations and data format for the ATHLET 3.4.2 code according to the manuals (Schöffel et al., 2024a), (Schöffel et al., 2024b), (Schöffel et al., 2024c).

The model contains the main components of the LDR 50: reactor, heat exchangers between the primary and the secondary sides, containment and water pool. The adopted nodalization is shown in Figure 38.

The reactor is represented by a core, a lower plenum, a riser, an upper plenum, a pressurizer, heat exchangers, and a downcomer. The core consist of three channals (central part, one fuel assembly with maximum energy release, peripheral part) and core bypass. The bottom of the fuel assemblies is considered to be located at a zero elevation of 0.0 m.

Heat release in the reactor core is simulated using heaters. Power distribution is implemented taking into account radial and axial power profiles Figure 39.

Co-funded by the European Union
UK Research and Innovation
The Research Council of Norway
Project funded by

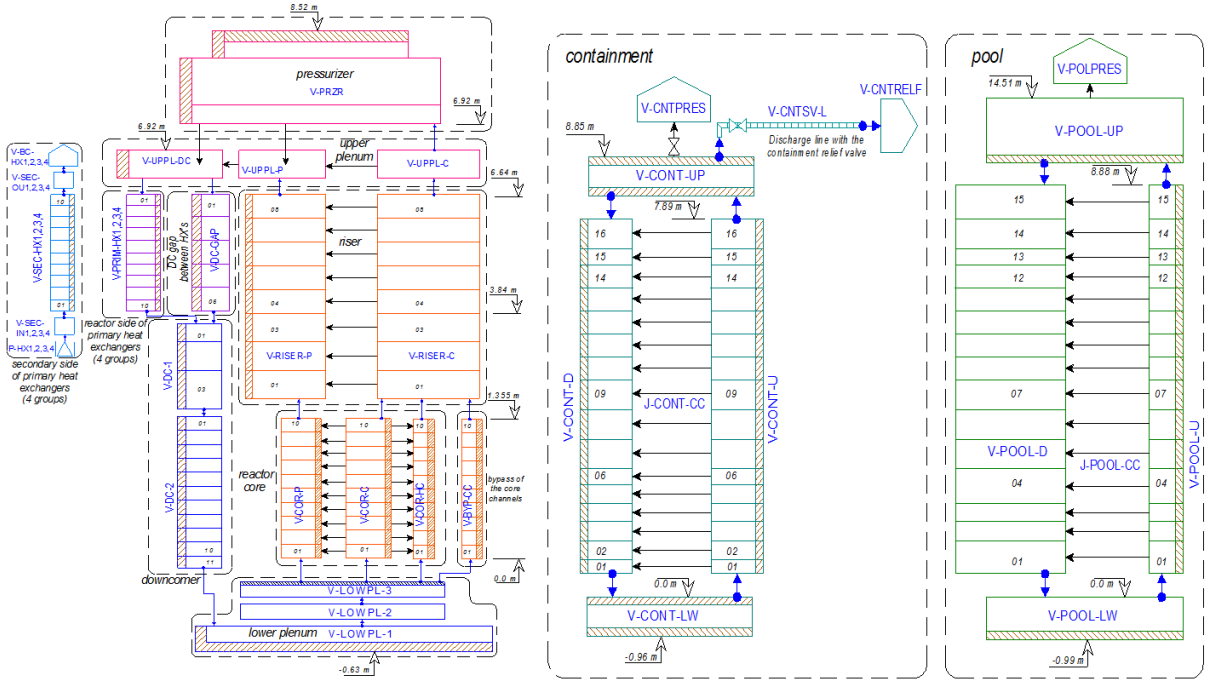

Figure 38. Nodalization of primary and secondary circuits, containment and pool in the ATHLET model.

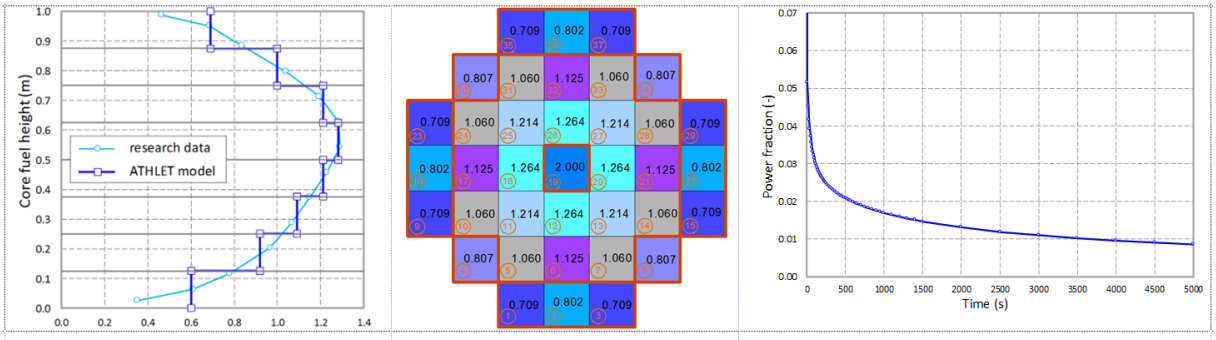

Axial power profile (K_z) | Radial power profile(K_q) | Decay heat after scram

Figure 39. Core power distribution in the ATHLET model.

Nodalization features	
Reactor vessel nodalization (1D or 3D)	1D
Reactor vessel number of vertical flow paths / radial rings and sectors	3
Axial levels in reactor vessel	24
Core model (1D or 3D)	1D
Number of hydraulic channels in core region (radial rings and sectors)	5
Axial levels in active core	10
Axial levels in the primary heat exchanger	10

Co-funded by the European Union
UK Research and Innovation
The Research Council of Norway
Project funded by

Number of secondary circuits modelled	1
Boundary conditions used in secondary circuit	Pressure, mass flow rate
District heating circuit modelled?	No
Total number of TH nodes in containment	4
Axial levels in containment	18
Total number of TH nodes in the pool	4
Axial levels in pool	17
Code options	
Choked flow model applied (e.g. Ramson-Trapp, Henry Fauske, etc.)	No
Specific models activated in PRZ (YES or NO and specify the model)	No
Specific models activated in containment (YES or NO and specify the model)	No
CCFL model (if activated, specify where in the primary system)	No
Dissolved nitrogen model (YES or NO and specify the model)	No

Parameter	Unit	Calculated
Hydraulic volumes		
Total primary circuit	m^3	40.984
Total secondary circuit	m^3	0.446
Containment	m^3	29.578
Pool	m^3	999,322
Elevations		
Primary circuit		
Reactor vessel bottom (inside of RPV)	m	-0.63
Core active region bottom (BAF)	m	0.0
Core active region top (TAF)	m	1.355
PRZ top (inside RPV)	m	8.52
HX inlet (active region)	m	6.64
HX outlet (active region)	m	3.84
Secondary circuit		
HX inlet (active region)	m	3.84
HX outlet (active region)	m	6.64
Containment		
Containment bottom	m	-0.96
Containment top	m	8.85
Pool		
Pool bottom	m	-0.96

Organization: ARB Analytical research bureau for NPP safety

Country: Ukraine

Code and version: COCOSYS 3.2.0.1

PC/operative system/compiler: Windows 10

Description of the code:

The COntainment COde SYStem (COCOSYS) has been developed by GRS (Gesellschaft für Anlagen und Reaktorsicherheit gGmbH) (Arndt, et al., 2023). The AC2 module COCOSYS provides a computer code on the basis of mechanistic models for the comprehensive simulation of all relevant processes and plant states during severe accidents in the containments of light water reactors, also covering the design basis accidents. One of the main aspects of this code system is the consideration of the interactions between the different processes. The code system can be used for the identification of possible deficits in plant safety, quantification of the safety reserves of the entire system, assessment of damage limiting or mitigating accident management measures, safety evaluation of new plant concepts.

In this work, COCOSYS is used to develop the LDR-50 Containment model and then for comprehensive simulation of anticipated transients (SBO) and design basis accidents (LOCA).

Description of the model:

The COCOSYS Containment model consists of the containment itself and water pool connected with environment. The thermal effect of the reactor vessel inside the containment is taken into account with boundary conditions. The containment is modelled with two columns of nodes and the water pool with three to maintain conditions for natural circulation. Heat removal from the water pool to the environment is simulated through the concrete walls and from the water surface. There is a containment relief valve (CRV) to protect the containment from excessive pressure. The COCOSYS Containment model developed to simulate the transient behavior of LDR-50 reactor is shown in Figure 40.

Boundary conditions for the steady-state and transient calculations are given by the near wall layer temperature distribution and heat transfer coefficient distribution (as functions of time) at the left surface of the heat structures that model the reactor vessel wall. Temperature and HTC distributions data as well as SBLOCA parameters (water, steam and nitrogen mass flow rates as well as enthalpy flows) were obtained from calculations of similar scenarios using the ATHLET code, performed by Energorisk.

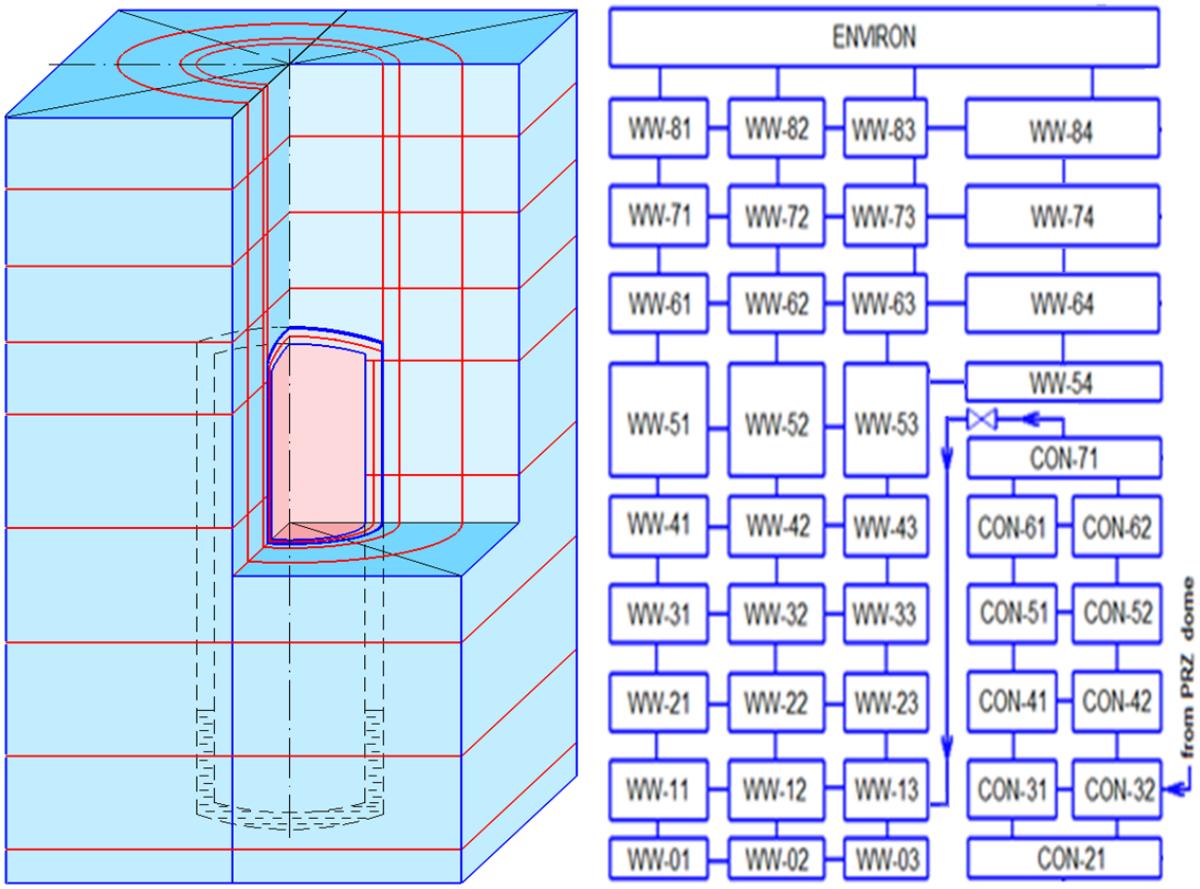

Figure 40. Schematic figure of ARB's COCOSYS model nodalization.

Nodalization features	
Model (1D or 3D)	1D
Number of vertical flow paths:Containment Water Pool	2 4
Number of axial levels:Containment Water Pool	6 9
Number of radial layers:Containment Water Pool	2 4
Total number of TH nodes: Containment Water Pool	10 32
Boundary conditions on the reactor side	Temperature

Parameter	**Unit**	**Calculated**
Hydraulic volumes		
Containment	m^3	27.667
Water Pool	m^3	998.546
Elevations		
Containment: bottom top	m	0.0 9.81

Co-funded by the European Union
UK Research and Innovation
The Research Council of Norway
Project funded by

Water Pool: bottom top	m	0.0 15.0

Co-funded by the European Union
UK Research and Innovation
The Research Council of Norway
Project funded by


EASI SMR